Statistical Computing on Riemannian manifolds

Applications in Medical Image Analysis

X. Pennec

INRIA SOPHIA ANTIPOLIS

EPIDAURE Project
2004, route des Lucioles B.P. 93
06902 Sophia Antipolis Cedex (France)

3-D Medical Images

MRI

X-Scan

Nuclear images

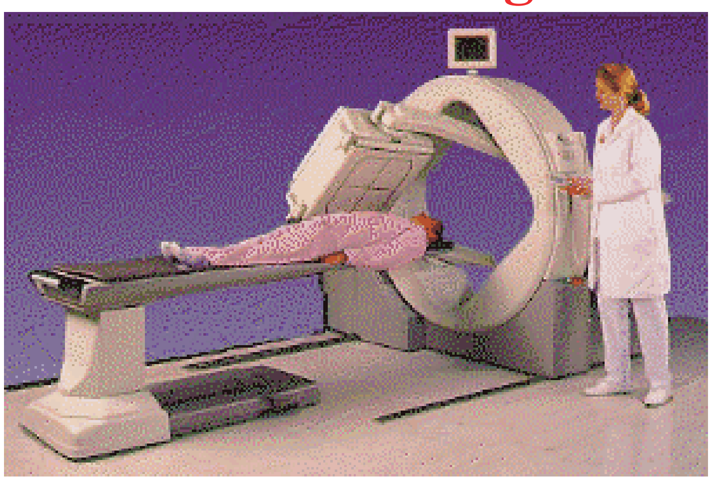

Echography

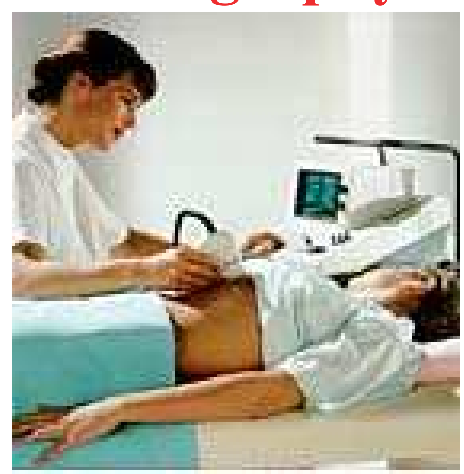

Complementary Images

MRI

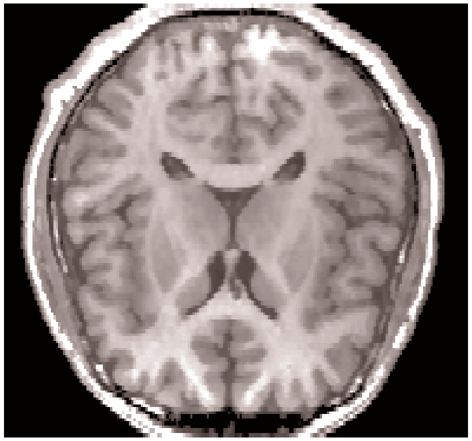

Anatomic

X-Scan

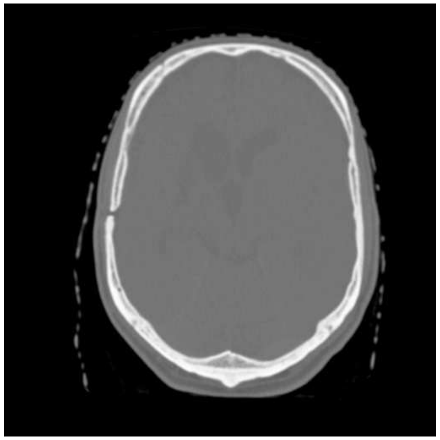

SPECT

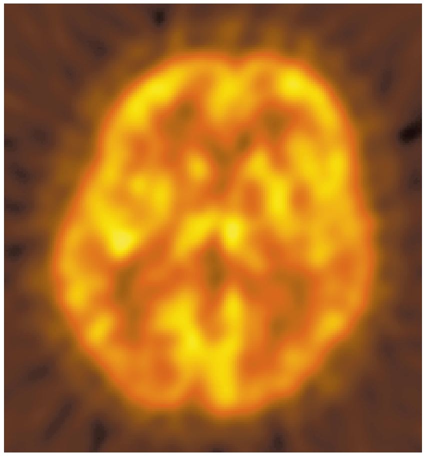

Functional

Echography

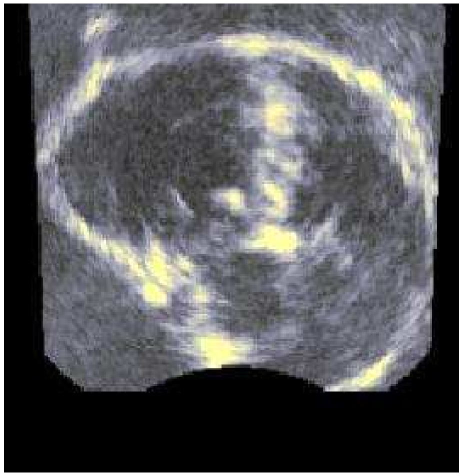

Medical Image analysis

To improve diagnosis

- quantitative and objective measures
- Image fusion and comparaison

To improve therapy

- planification (before)
- control (during)
- evaluation (after)

Medical Image Analysis

Measures are geometric and noisy

- Registration = determine a transformations
- Diffusion tensor imaging
- Feature extracted from images

We need:

- Statistics
- A stable computing framework

MR/US registration of per-operative images

MR Image

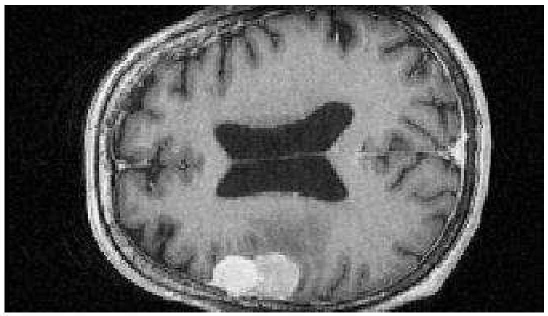

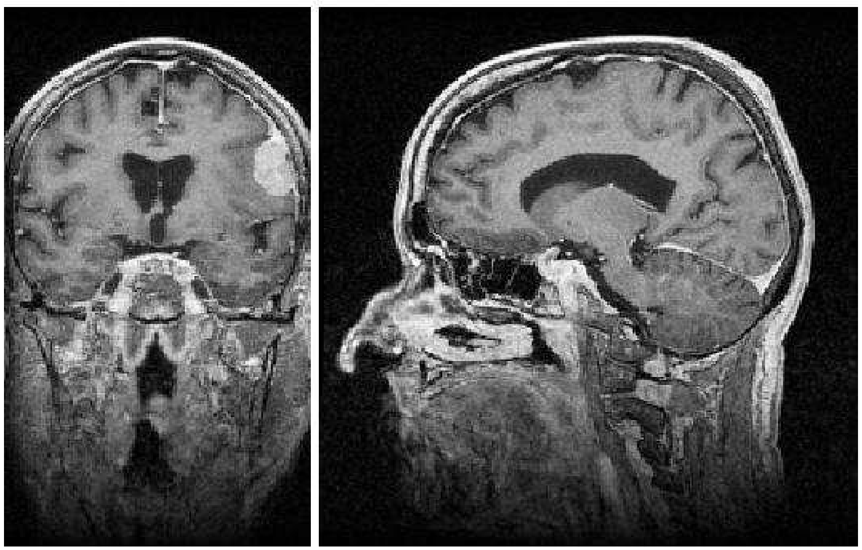

Registered US

Initial US

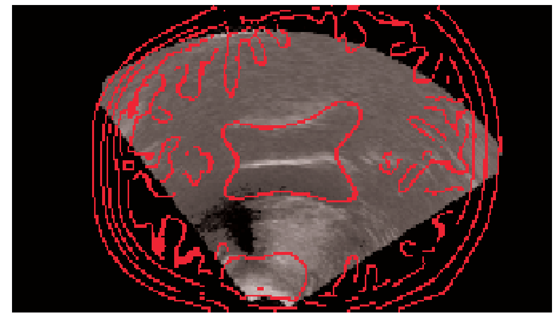

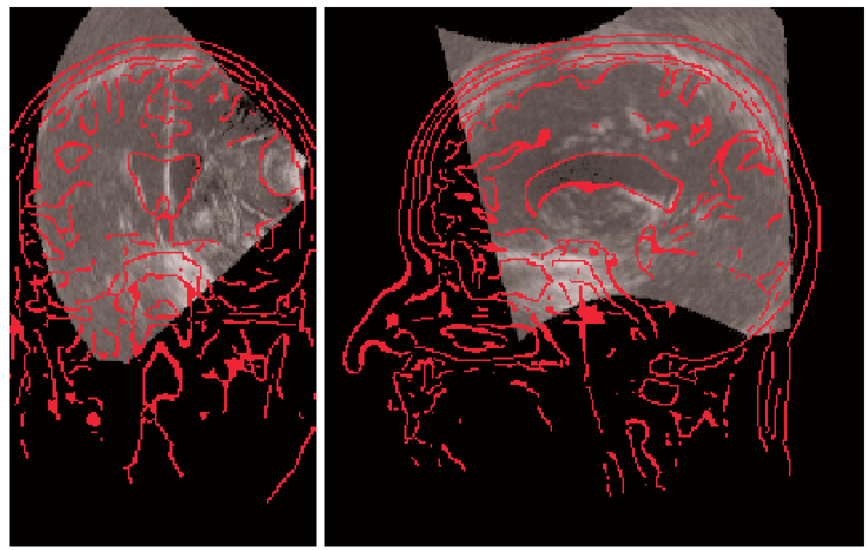

Variability of a registration algorithm

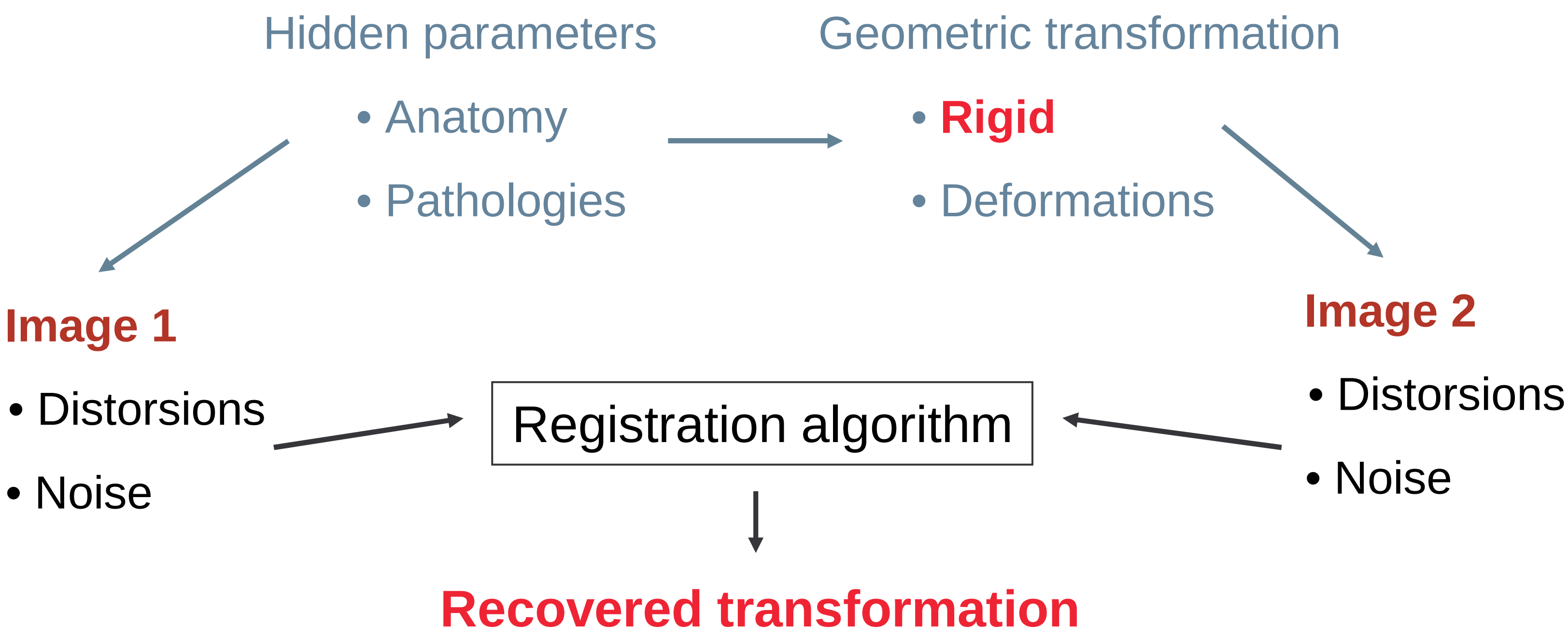

Quantify the statistical Variability of the transformation:

- Mean value (bias)
- Covariance matrix, std dev. (accuracy, precision)
  - On the transformation (rotation σ_r [rad], translation σ_t [mm])
  - Propagate on target points (TRE σ_x)

Diffusion Tensor Imaging:
3D Fields of Symmetric positive definite matrices

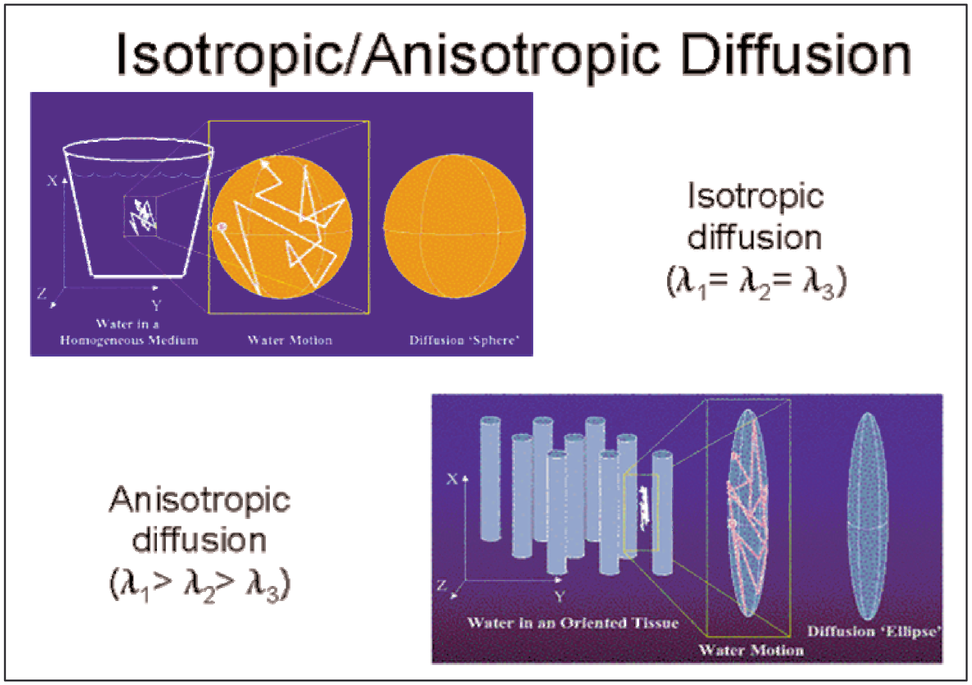

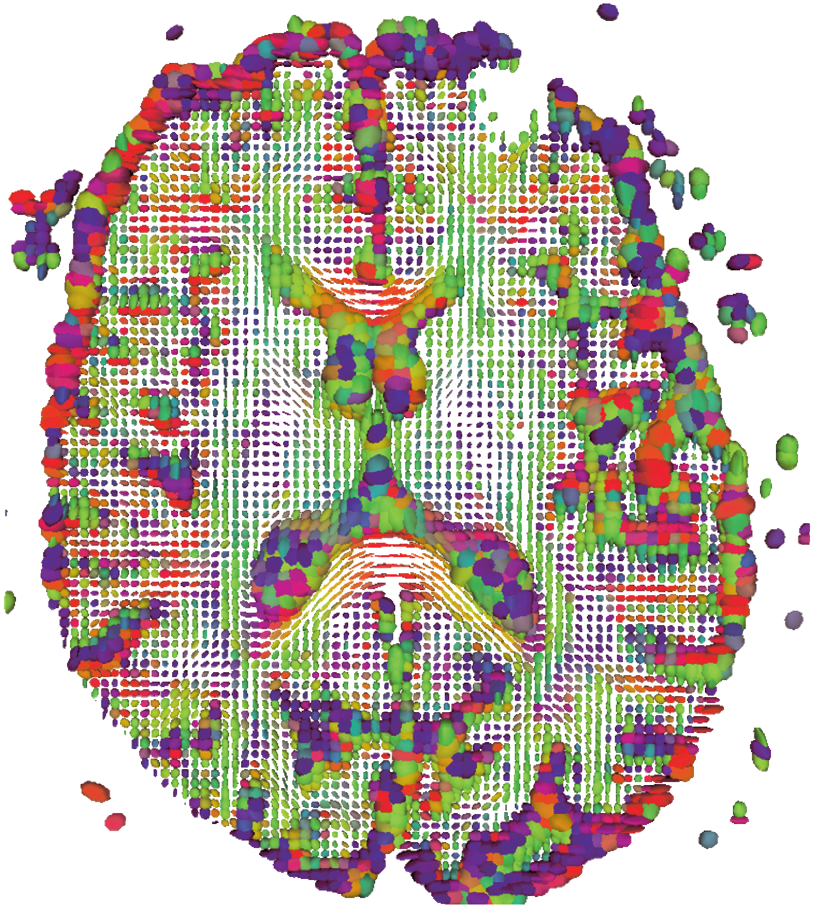

DTI Tensor field (slice of a 3D volume)

Tensor computing in DTI

Very noisy data

Preprocessing steps

- Filtering
- Regularization
- Robust estimation

Processing steps

- Interpolation / extrapolation
- Statistical comparisons

Can we generalize scalar methods?

- Linear convex combinations are stable (mean, interpolation)
- More complex methods are not (null or negative eigenvalues)
  - Linear estimation of the tensor field from images
  - Gradient descent
  - Anisotropic filtering and diffusion

Example of geometrical objects

Geometric features

- Lines, oriented points, tensors
- Amino Acids: frames
- Extremal points: semi-oriented frames

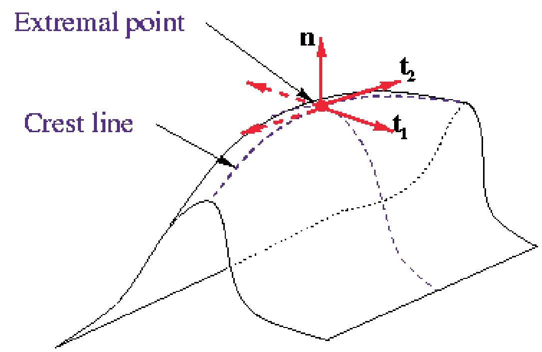

Transformations

- Affine, projective… rigid 3D

Basic probabilities and statistics

Measure: random vector x of pdf $p_{\mathbf{x}}(z)$

Approximation: $\mathbf{x} \sim (\overline{\mathrm{x}}, \mathbf{\Sigma}_{\mathbf{xx}})$

- Mean: $\overline{\mathrm{x}} = \mathrm{E}(\mathbf{x}) = \int z.p_{\mathbf{x}}(z).dz$
- Covariance: $\Sigma_{\mathbf{xx}} = \mathrm{E}\left[(\mathbf{x}-\overline{\mathrm{x}}).(\mathbf{x}-\overline{\mathrm{x}})^T\right]$

Propagation:

$$\mathbf{y} = h(\mathbf{x}) \sim \left(h(\overline{\mathrm{x}}),\ \frac{\partial h}{\partial \mathrm{x}}.\mathbf{\Sigma}_{\mathbf{xx}}.\frac{\partial h}{\partial \mathrm{x}}^{\mathrm{T}} \right)$$

Noise model: additive, Gaussian...

Statistical distance: Mahalanobis and χ^2

Some problems with geometric features

Mean of 3D rotations:

invariance w.r.t. the chart

$$\underline{\mathbf{R}} = \frac{1}{n}\sum_i \mathbf{R}_i \qquad \underline{q} = \frac{1}{n}\sum_i q_i \qquad \underline{r} = \frac{1}{n}\sum_i r_i$$

Noise on 3D rotations:

invariance w.r.t. the transformation group

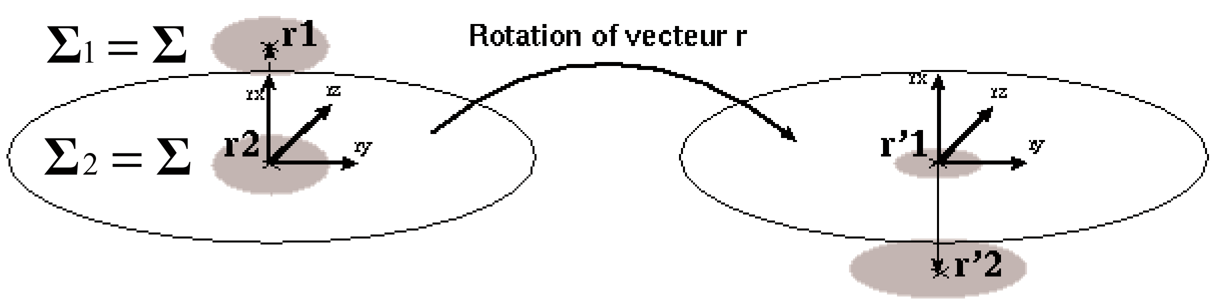

$$\Sigma_1' = \frac{8}{\pi^2}\Sigma$$

$$\Sigma_2' = \frac{\pi^2}{8}\Sigma$$

$$\Sigma = \sigma^2 \begin{bmatrix} 0 & 0 & 0 \\ 0 & 1 & 0 \\ 0 & 0 & 1 \end{bmatrix}$$

Overview

- ➔ **Statistics on Riemannian manifolds**
  - ⇨ **The Riemannian framework**
  - Choice of the metric and invariance properties
- **Registration performances**
- **Tensor computing**
- **Conclusion**

Statistics on Riemannian Manifolds

Riemannian metric :

- Dot product on tangent space
- Speed, length of a curve
- Distance and geodesics
  (angle, great circles)

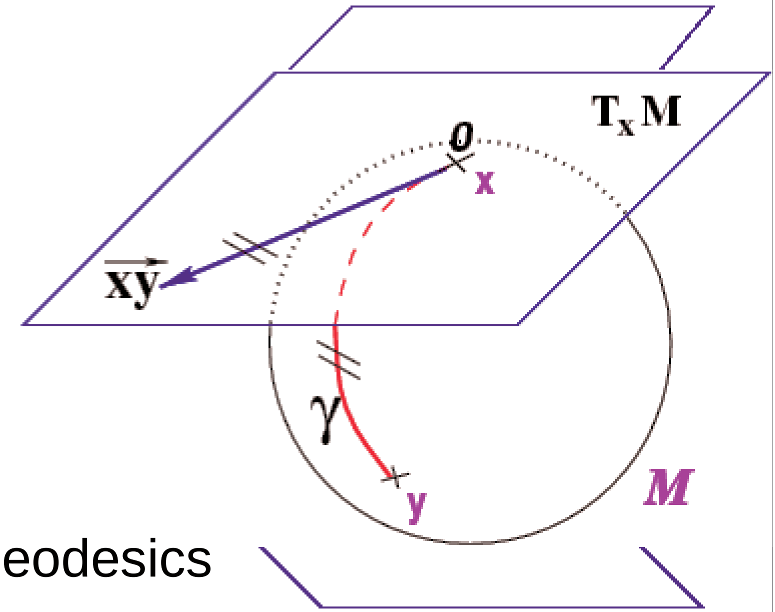

Exponential chart (Normal coord. syst.) :

- Development in tangent space along geodesics
- Geodesics = straight lines
- Distance = Euclidean
- Star shape domain limited by the cut-locus
- Covers all the manifold if geodesically complete

Probabilities

Volume form

$$\langle w, v \rangle_{\mathrm{x}} = w^T . Q(x) . v \quad \Rightarrow \quad d\mathrm{M}(\mathrm{x}) = \sqrt{|\, Q(x) \,|} . dx$$

Probility density functions

$$\forall X, P(x \in X) = \int_X p_{\mathbf{x}}(y) . d\,\mathrm{M}(y) \qquad \text{with} \qquad P(\mathrm{M}) = 1$$

Expectation of an observable $\phi : \mathrm{M} \to \mathrm{R}$

$$\mathrm{E}[\phi(x)] = \int_{\mathrm{M}} \phi(y) . p_{\mathbf{x}}(y) . d\mathrm{M}(y)$$

Variance w.r.t. a fixed primitive

$$\sigma_{\mathbf{x}}^2(y) = \mathrm{E}\left[\operatorname{dist}(y, \underline{\mathrm{x}})^2\right] = \int_{\mathrm{M}} \operatorname{dist}(y, z)^2 . p_{\mathbf{x}}(z) . d\mathrm{M}(z)$$

Probabilities

Metric -> Volume forme (measure) $d\mathrm{M}(\mathrm{x})$

Probility density functions $\forall X, P(x \in X) = \int_X p_{\mathbf{x}}(y).d\,\mathrm{M}(y)$

Expectation of a function ϕ from M into R :

- Definition : $\mathrm{E}[\phi(x)] = \int_{\mathrm{M}} \phi(y).p_{\mathbf{x}}(y).d\mathrm{M}(y)$
- Variance : $\sigma_{\mathbf{x}}^2(y) = \mathrm{E}\left[\mathrm{dist}(y, \underline{\mathrm{x}})^2\right] = \int_{\mathrm{M}} \mathrm{dist}(y, z)^2.p_{\mathbf{x}}(z).d\mathrm{M}(z)$
- Information : $\mathrm{I}[\mathbf{x}] = \mathrm{E}[\log(p_{\mathbf{x}}(\mathbf{x}))]$

Fréchet expectation (1944)

Minimizing the variance

$$\mathrm{E}[\mathbf{x}] = \underset{y \in \mathrm{M}}{\operatorname{argmin}} \left(\mathrm{E}\left[\operatorname{dist}(y, \mathbf{x})^2 \right] \right)$$

- **Existence and uniqueness : Karcher and Kendall**

Characterization as an exponential barycenter (P(C)=0)

$$\operatorname{grad}\left(\sigma_{\mathbf{x}}^2(y)\right) = 0 \quad \Rightarrow \quad \mathrm{E}\left[\overrightarrow{\bar{\mathrm{x}}\mathbf{x}}\right] = \int_{\mathrm{M}} \overrightarrow{\bar{\mathrm{x}}\mathbf{x}}.p_{\mathbf{x}}(z).d\mathrm{M}(z) = 0$$

The case of points: classical expectation $\bar{\mathrm{x}} \in \mathrm{E}[\mathbf{x}] \quad \Rightarrow \quad \mathrm{E}[-\bar{\mathrm{x}} + \mathbf{x}] = 0$

Other central primitives

$$\mathrm{E}^{\alpha}[\mathbf{x}] = \underset{y \in \mathrm{M}}{\operatorname{argmin}} \left(\mathrm{E}\left[\operatorname{dist}(y, \mathbf{x})^{\alpha} \right] \right)^{1/\alpha}$$

[Pennec, INRIA Research Report RR-5093]

A gradient descent (Gauss-Newton) algorithm

Vector space

$$f(x+v) = f(x) + \nabla f^T . v + \tfrac{1}{2} v^T . H_f . v$$

$$x_{t+1} = x_t + v \quad \text{with} \quad v = -H_f^{(-1)} . \nabla f$$

Manifold

$$f(\exp_x(v)) = f(x) + \nabla f(v) + \tfrac{1}{2} H_f(v,v)$$

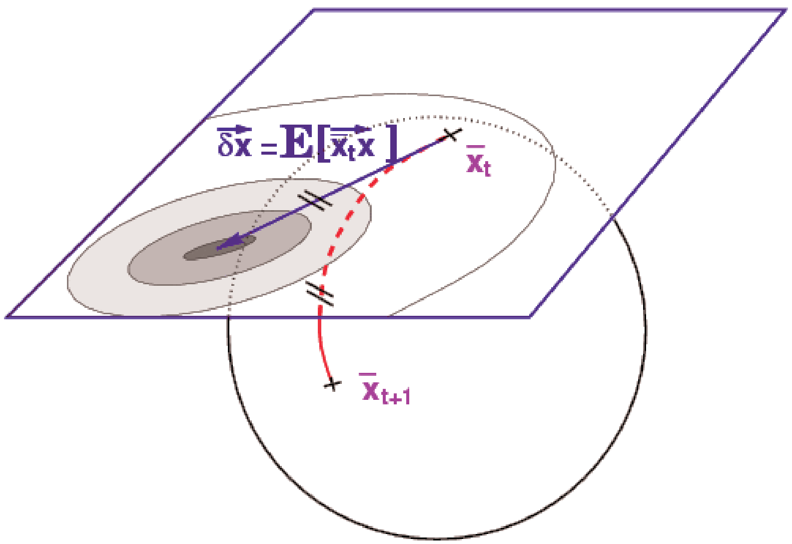

$$\nabla\left(\sigma_{\mathbf{x}}^2(\mathrm{y})\right) = -2\,\mathrm{E}\left[\overrightarrow{\mathrm{y}\mathbf{x}}\right] = \frac{-2}{n} \sum_i \overrightarrow{\mathrm{y}\mathrm{x}_i}$$

$$H_{\sigma_{\mathbf{x}}^2} \approx 2Id$$

Geodesic marching

$$\bar{\mathrm{x}}_{t+1} = \exp_{\bar{\mathrm{x}}_t}(v) \quad \text{with} \quad v = \mathrm{E}\left[\overrightarrow{\mathrm{y}\mathbf{x}}\right]$$

Covariance matrix

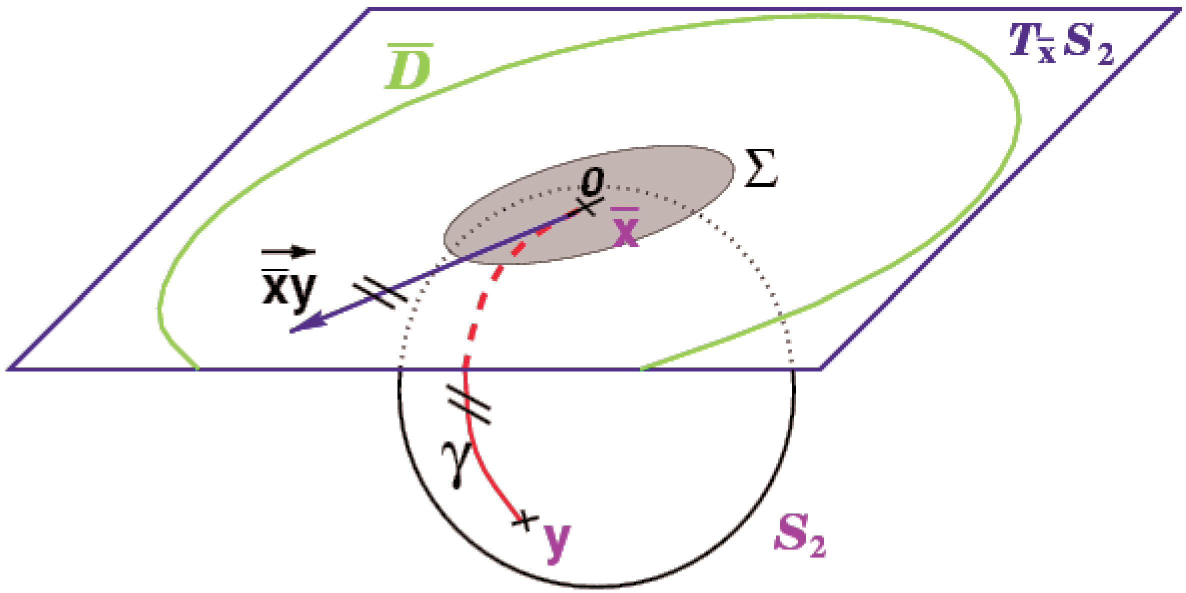

$$E\left[\overrightarrow{\bar{x}\mathbf{x}}\right] = \int_{M} \overrightarrow{\bar{x}\mathbf{x}}.p_{\mathbf{x}}(z).dM(z) = 0$$

$$\Sigma_{\mathbf{xx}} = E\left[\left(\overrightarrow{\bar{x}\mathbf{x}}\right).\left(\overrightarrow{\bar{x}\mathbf{x}}\right)^{T}\right] = \int_{M} \left(\overrightarrow{\bar{x}z}\right).\left(\overrightarrow{\bar{x}z}\right)^{T}.p_{\mathbf{x}}(z).dM(z) = 0$$

Uniform and Gaussian pdf

Practical approximation $\mathbf{x} \sim (\bar{\mathrm{x}}, \mathbf{\Sigma}_{\mathbf{xx}})$

Information of a pdf $\mathrm{I}[\mathbf{x}] = \mathrm{E}[\log(p_{\mathbf{x}}(\mathbf{x}))]$

Uniform distribution

$$\min_{\mathbf{x}} \left(\mathrm{I}[\mathbf{x}] \mid \mathbf{x} \in X\right)$$

$$p_{\mathbf{x}}(z) = \mathrm{Ind}_X(z) / \mathrm{Vol}(X)$$

Gaussian distribution

$$\min_{\mathbf{x}} \left(\mathrm{I}[\mathbf{x}] \mid \mathrm{E}[\mathbf{x}] = \bar{\mathrm{x}},\ \mathbf{\Sigma}_{\mathbf{xx}} = \mathbf{\Sigma}\right)$$

$$N(y) = k.\exp\left(\left(\overrightarrow{\bar{\mathrm{x}}\mathbf{x}}\right)^{\mathrm{T}} .\mathbf{\Gamma}.\left(\overrightarrow{\bar{\mathrm{x}}\mathbf{x}}\right) / 2\right)$$

$$\mathbf{\Gamma} = \mathbf{\Sigma}^{(-1)} - \tfrac{1}{3}\mathrm{Ric} + O(\sigma) + \varepsilon(\sigma / r)$$

$$k = (2\pi)^{-n/2}.\det(\mathbf{\Sigma})^{-1/2}.\left(1 + O(\sigma^3) + \varepsilon(\sigma / r)\right)$$

Some distributions

Uniform density:

- maximal entropy knowing X

$$p_{\mathbf{x}}(z) = \mathrm{Ind}_X(z) / \mathrm{Vol}(X)$$

Gaussian density:

- maximal entropy knowing the mean and the covariance

$$N(y) = k.\exp\left(\left(\overrightarrow{\bar{\mathrm{x}}\mathbf{x}} \right)^{\mathrm{T}} .\boldsymbol{\Gamma}. \left(\overrightarrow{\bar{\mathrm{x}}\mathbf{x}} \right) / 2 \right)$$

$$\boldsymbol{\Gamma} = \boldsymbol{\Sigma}^{(-1)} - \tfrac{1}{3}\mathrm{Ric} + O(\sigma) + \varepsilon(\sigma / r)$$

$$k = (2\pi)^{-n/2}.\det(\boldsymbol{\Sigma})^{-1/2}.\left(1 + O(\sigma^3) + \varepsilon(\sigma / r)\right)$$

Mahalanobis distance:

$$\mu_{\mathbf{x}}^2(\mathrm{y}) = \overrightarrow{\bar{\mathrm{x}}\mathrm{y}}^{\,t} .\Sigma_{\mathbf{xx}}^{(-1)} .\overrightarrow{\bar{\mathrm{x}}\mathrm{y}}$$

- Any distribution:

$$\mathrm{E}\left[\mu_{\mathbf{x}}^2(\mathbf{x})\right] = n$$

- Gaussian:

$$\mathrm{E}\left[\mu_{\mathbf{x}}^2(\mathbf{x})\right] = \chi_n^2 + O(\sigma^3) + \varepsilon\left(\frac{\sigma}{r}\right)$$

Gaussian on the circle

Exponential chart: $x = r\theta \in \,]-\pi.r\,;\pi.r[$

Gaussian: truncated standard Gaussian

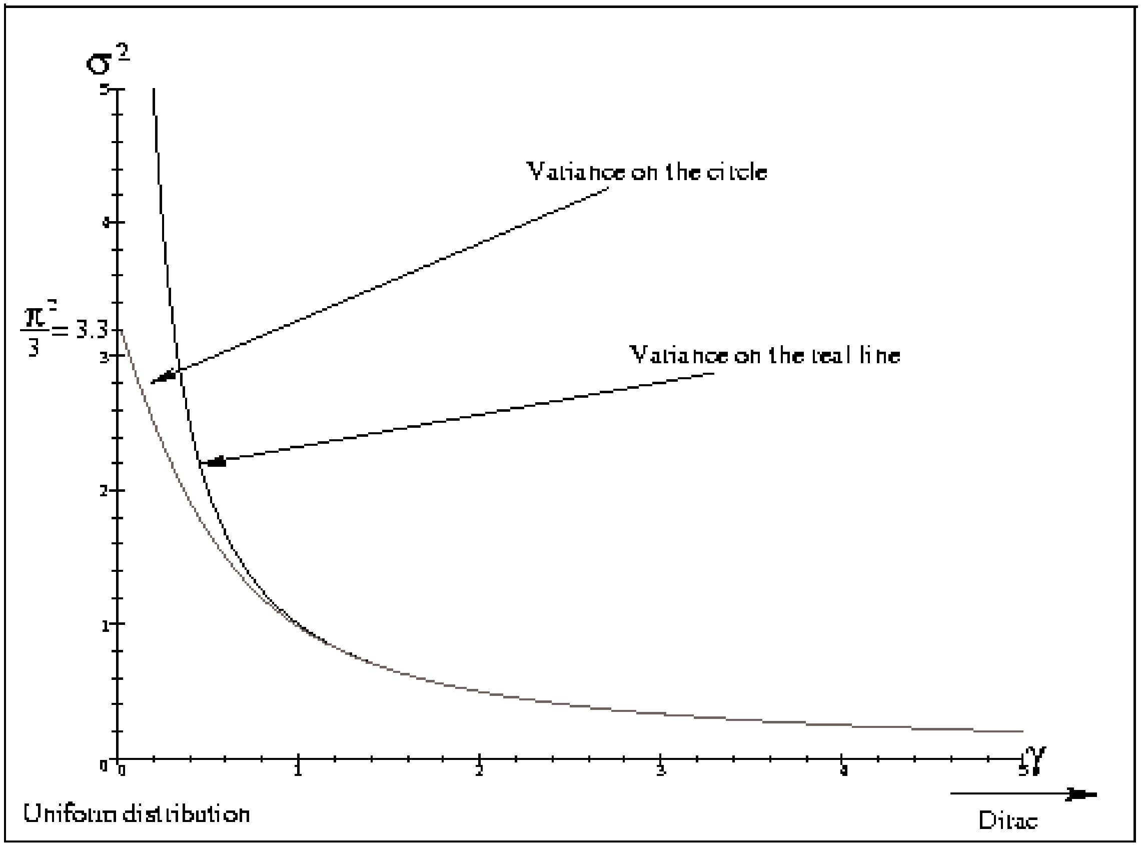

$r \to \infty$: standard Gaussian

$\gamma \to 0$: uniform pdf with

$$\sigma^2 = (\pi.r)^2 / 3$$

$\gamma \to \infty$: Dirac

Metric choice on Transformation (Lie) Group

Metric choice: left invariant $\mathrm{dist}(g,h) = \mathrm{dist}(f \circ g, f \circ h)$

- The principal chart (exp. chart at the origin) can be translated at any point : only one chart.

$$\mathrm{dist}(g,h) = \left\| \overrightarrow{f^{(-1)} \circ \vec{g}} \right\|$$

Practical computations $\overrightarrow{fg} = g - f \quad \Leftrightarrow \quad \overrightarrow{fg} = f^{(-1)} \circ g$

$$f + \overrightarrow{\delta f} \quad \Leftrightarrow \quad \exp_{\vec{f}}\left(\overrightarrow{\delta f}\right) = f \circ \overrightarrow{\delta f}$$

- Atomic operations $\left[\vec{f} \circ \vec{g}\right]$, $\left[\overrightarrow{f^{(-1)}}\right]$ and their Jacobian

Metric choice on Homogeneous manifolds

Metric choice: invariant $\text{dist}(x, y) = \text{dist}(g * x, g * y)$

- Isotropy group of the origin: $H = \{h * o = o\}$
- Existance condition: $\text{dist}(x, o) = \text{dist}(h * x, o)$
- Placement function: $f_x * o = x$

Practical computations $\overrightarrow{xy} = y - x \quad \Leftrightarrow \quad \overrightarrow{xy} = f_x^{(-1)} * \vec{y}$

$$x + \overrightarrow{\delta x} \quad \Leftrightarrow \quad \exp_x\left(\overrightarrow{\delta x}\right) = f_x * \overrightarrow{\delta x}$$

- Atomic operations $\left[f * \vec{x}\right], \ \left[f_x\right]$ and their Jacobian

A few properties of the pdfs

Invariant measure (Haar):

$$d\,\mathrm{M}(\mathrm{f} * \mathrm{x}) = d\,\mathrm{M}(\mathrm{x})$$

Action on a random feature

- The mean is equivariant
- The pdf is translated by

$$p_{(\mathrm{f} * \mathbf{x})}(\mathrm{y}) = p_{\mathbf{x}}(\mathrm{f}^{(-1)} * \mathrm{y})$$

$$\left[\quad p_{(z+\mathbf{x})}(\mathrm{y}) = p_{\mathbf{x}}(-z + \mathrm{y}) \quad \right]$$

Composition of random transformations

- The mean is left-equivariant (but generally not right-equivarient)
- The pdf is an (asymetric) convolution product

$$p_{(\mathbf{f}_1 \circ \mathbf{f}_2)}(\mathrm{f}) = \int_{\mathrm{G}} p_{\mathbf{f}_1}(\mathrm{g}).p_{\mathbf{f}_2}(\mathrm{g}^{(-1)} \circ \mathrm{f}).d_L\,\mathrm{G}(\mathrm{g})$$

$$\left[\quad p_{(\mathbf{x}+\mathbf{y})}(z) = \left(p_{\mathbf{x}} \otimes p_{\mathbf{y}}\right)(z) = \int p_{\mathbf{x}}(t).p_{\mathbf{y}}(z-t).dt \quad \right]$$

Example with 3D rotations

Principal chart: rotation vector : $r = \theta . n$

Distance: $\mathrm{dist}(R_1, R_2) = \left\| r_1^{(-1)} \circ r_2 \right\|$

Frechet mean:

$$\overline{R} = \arg\min_{R \in SO_3} \left(\sum_{i} \mathrm{dist}(R, R_i) \right)$$

Centered chart:

mean = barycenter

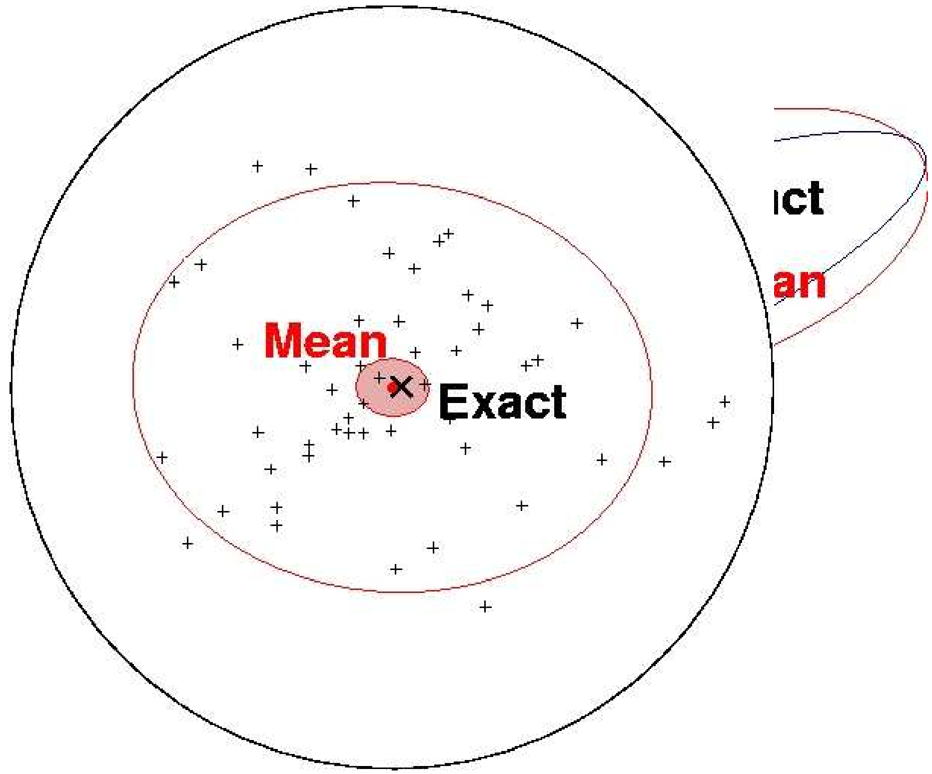

Overview

- ✓ **Statistics on Riemannian manifolds**
- ⇨ **Registration performances**
  - Error prediction for landmark-based registration
  - Performance evaluation for iconic and surface and intensity-based methods
- **Tensor computing**
- **Conclusion**

Registration of Images

Goal = finding correspondences between homologous points (duality matches / transformation)

Feature space

- 0D: points, landmarks, frames
- 1D: curves
- 2D: surfaces
- 3D: volumes (i.e. intensity-based methods)

Transformation space

- Rigid, affine, locally affine, deformable
- Dimensionality reduction (e.g. 3D/2D)

Similarity metric (criterion), optimization scheme

Uncertainty of feature-based registration

Matches estimation

- Alignment
- Geometric hashing
- ICP

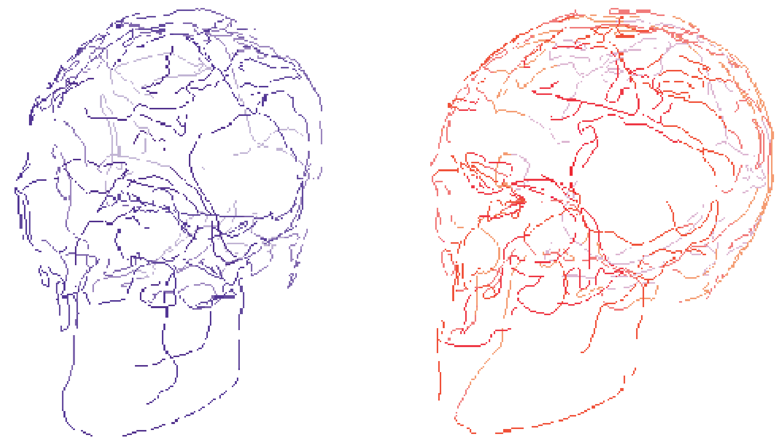

Least square registration

$$C(T,\chi) = \sum_i \left\| y_i - T * x_i \right\|^2$$

- Propagation of the errors from the data to the optimal transformation at the first order (implicit function theorem):

$$\Sigma_{\chi\chi} = \sigma^2.Id \quad \Rightarrow \quad \boxed{\Sigma_{TT} = \sigma^2.H^{-1}} \quad \text{with} \quad H = \frac{\partial^2 C(T,\chi)}{\partial T^2}$$

Registration of CT images of a dry skull

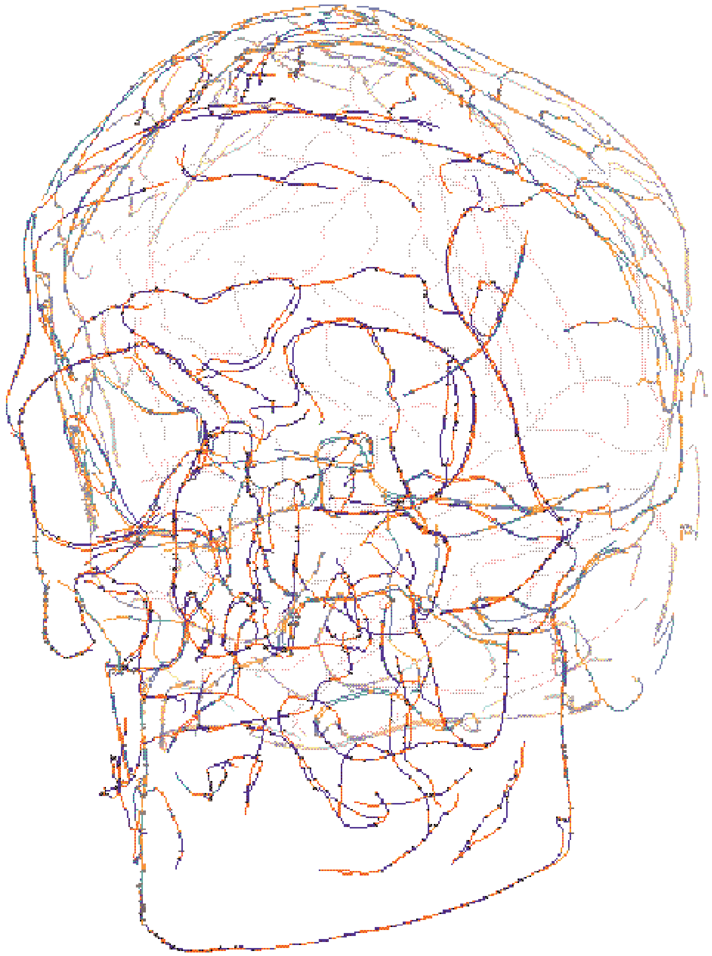

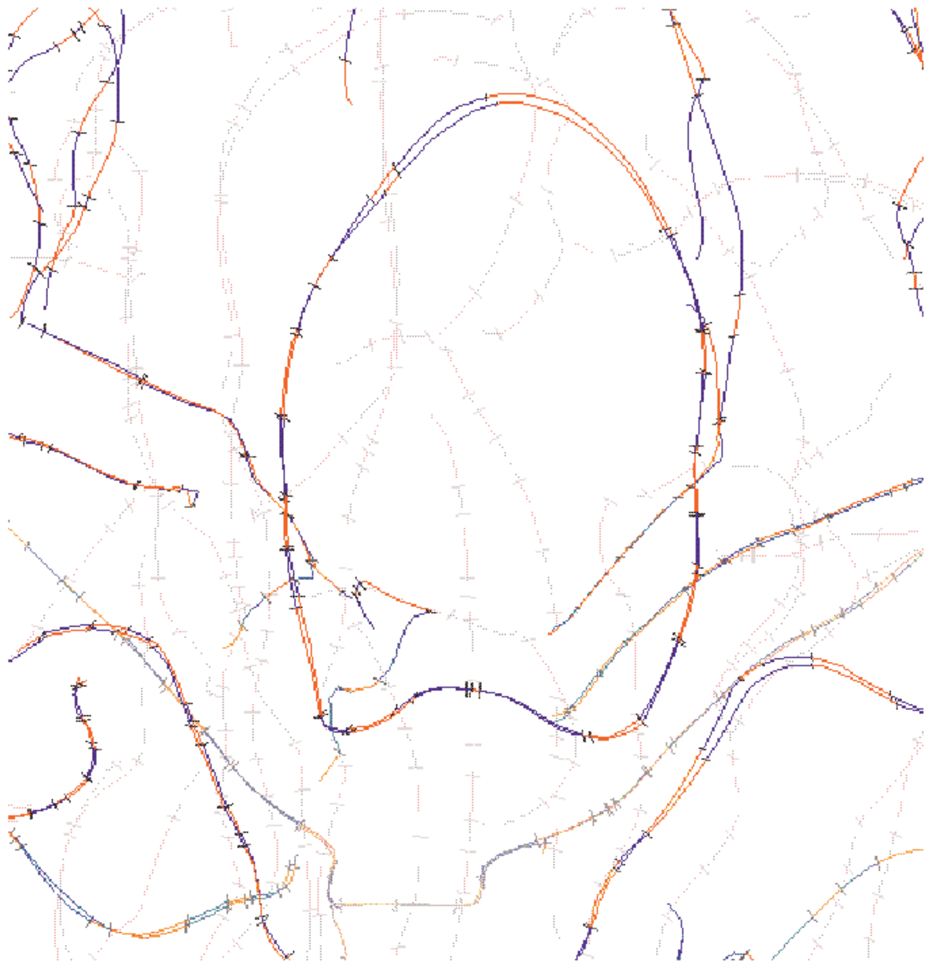

550 matched frames among 2000

Typical object accuracy: 0.04 mm

Typical corner accuracy: 0.10 mm

Registration of MR T1 images of the head

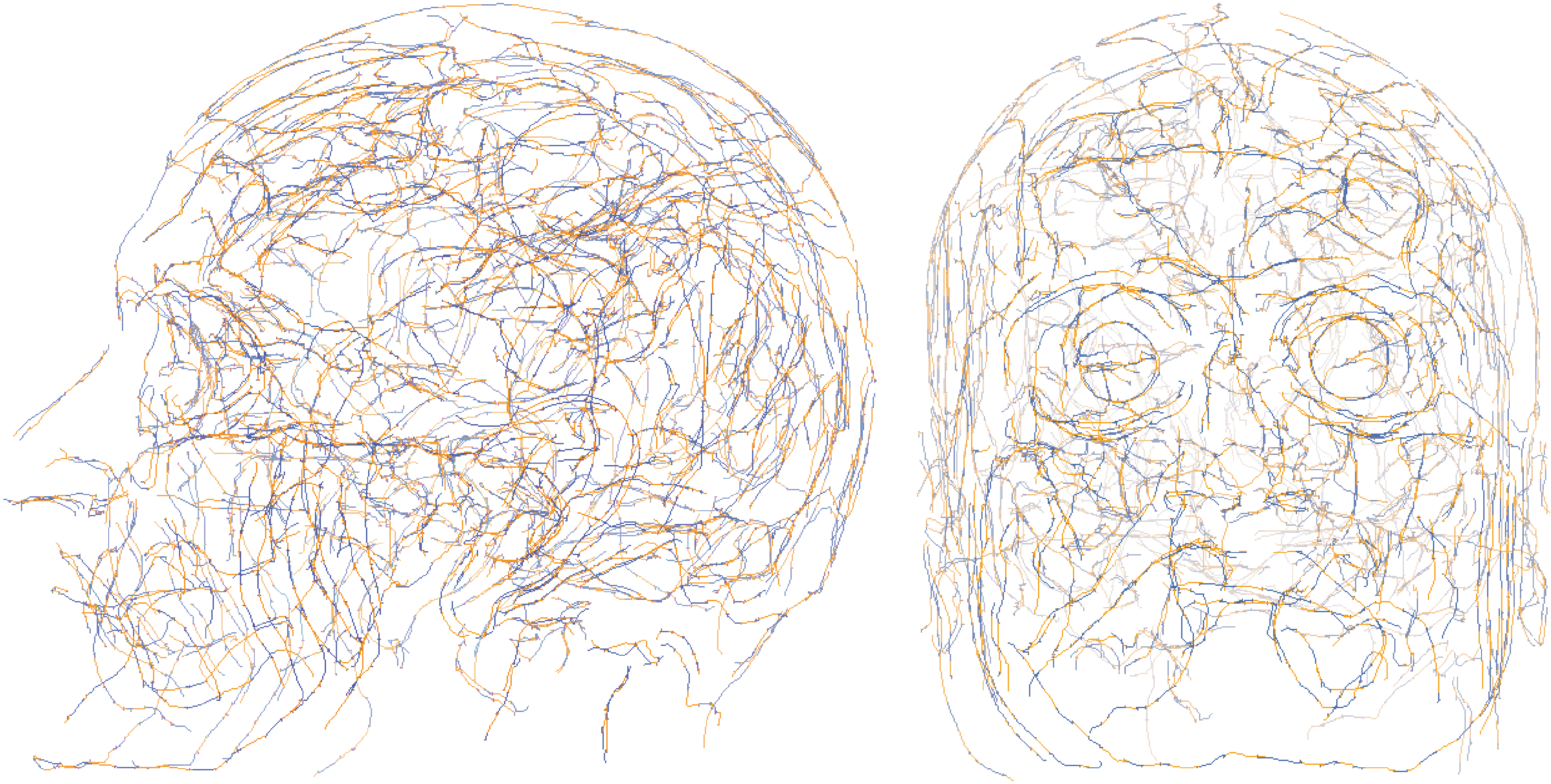

Typical object accuracy: 0.06 mm

860 matched frames among 3600

Typical corner accuracy: 0.125 mm

Validation of the accuracy evaluation

Brigham and Women's Multiple Sclerosis database

- 24 acquisitions 3D per patient on 1 year
- T2 weighted MR, 2 echo times, voxels 1 x 1 x 3 mm

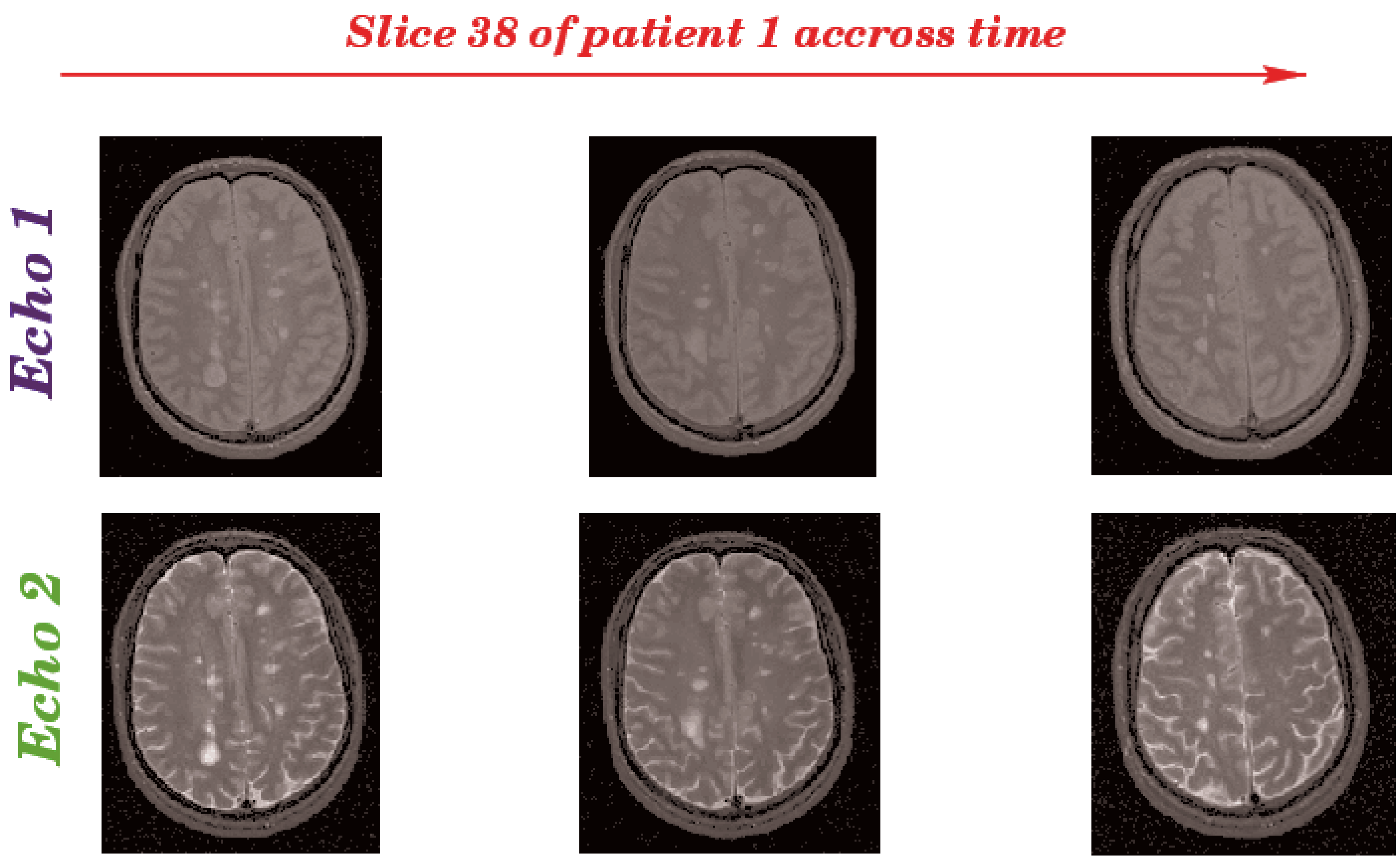

Validation of the accuracy evaluation

Brigham and Women's Multiple Sclerosis database

- 24 acquisitions 3D per patient on 1 year
- T2 weighted MR, 2 echo times, voxels 1 x 1 x 3 mm

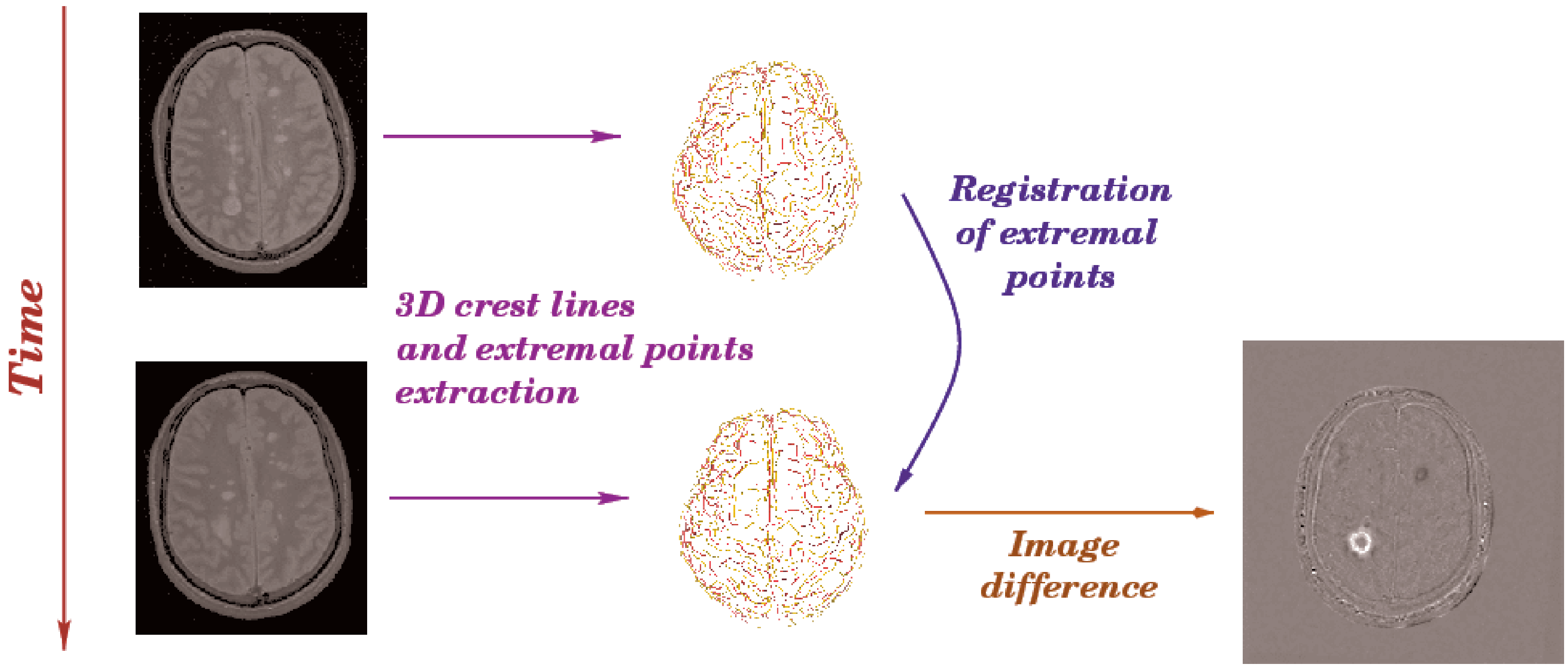

Predicted object accuracy: 0.06 mm.

Validation of the accuracy evaluation

Brigham and Women's Multiple Sclerosis database

- 24 acquisitions 3D per patient on 1 year
- T2 weighted MR, 2 echo times, voxels 1 x 1 x 3 mm

Visualization of the signal evolution: one image line across time

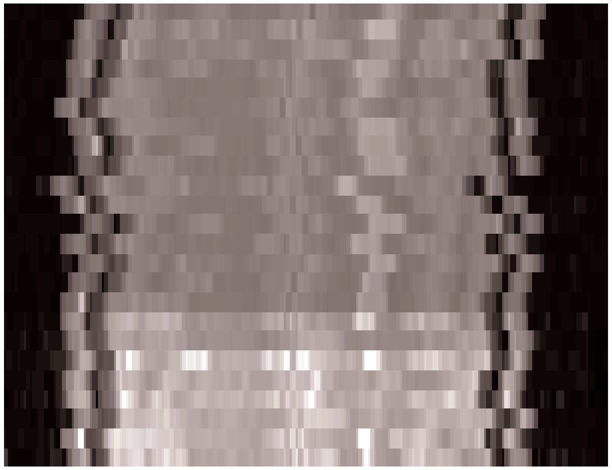

Without registration

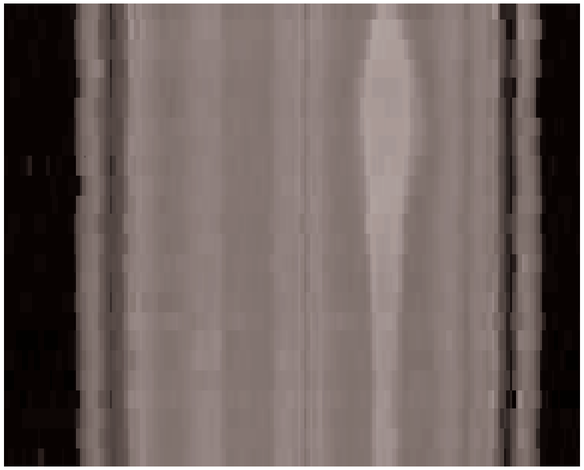

After registration

and intensity correction

Validation of the accuracy with double echoes

Comparing two transformations and their Covariance matrix :

$$\mu^2(T_1, T_2) \approx \chi_6^2$$

Mean: 6, Var: 12

KS test

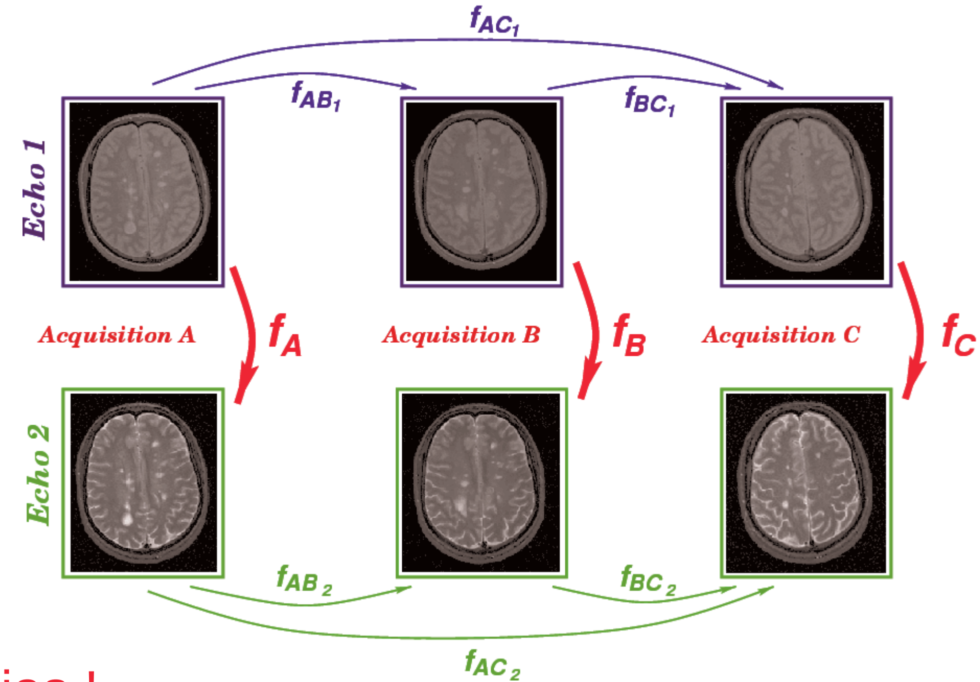

Intra-echo: $\mu^2 \approx 6$, KS test OK

Inter-echo: $\mu^2 > 50$, KS test failed, Bias !

Bias esimation: (chemical shift, susceptibility effects)

- $\sigma_{rot} = 0.06 \ \deg$ (not significantly different from the identity)
- $\sigma_{trans} = 0.2 \ \mathrm{mm}$ (significantly different from the identity)

Inter-echo with bias corrected: $\mu^2 \approx 6$, KS test OK

[X. Pennec et al., Int. J. Comp. Vis. 25(3) 1997, MICCAI 1998]

Overview

- ✓ **Statistics on Riemannian manifolds**
- ⇨ **Registration performances**
  - ✓ Error prediction for landmark-based registration
  - ⇨ A posteriori consistency evaluation
- ❍ **Tensor computing**
- ❍ **Conclusion**

Roboscope: per-operative MR/US registration

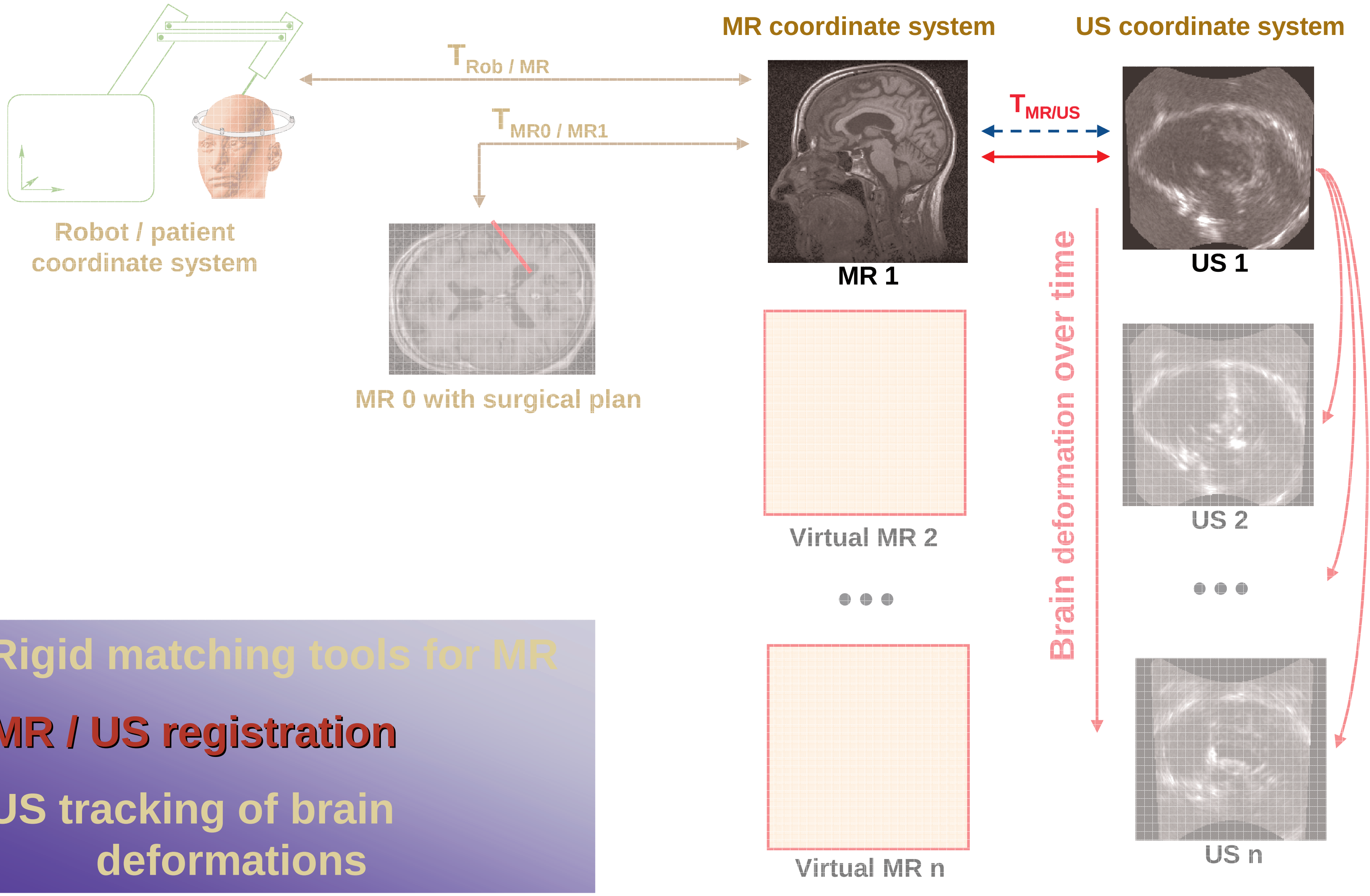

- Rigid matching tools for MR
- **MR / US registration**
- US tracking of brain deformations

Registration of MR/US images

MR image

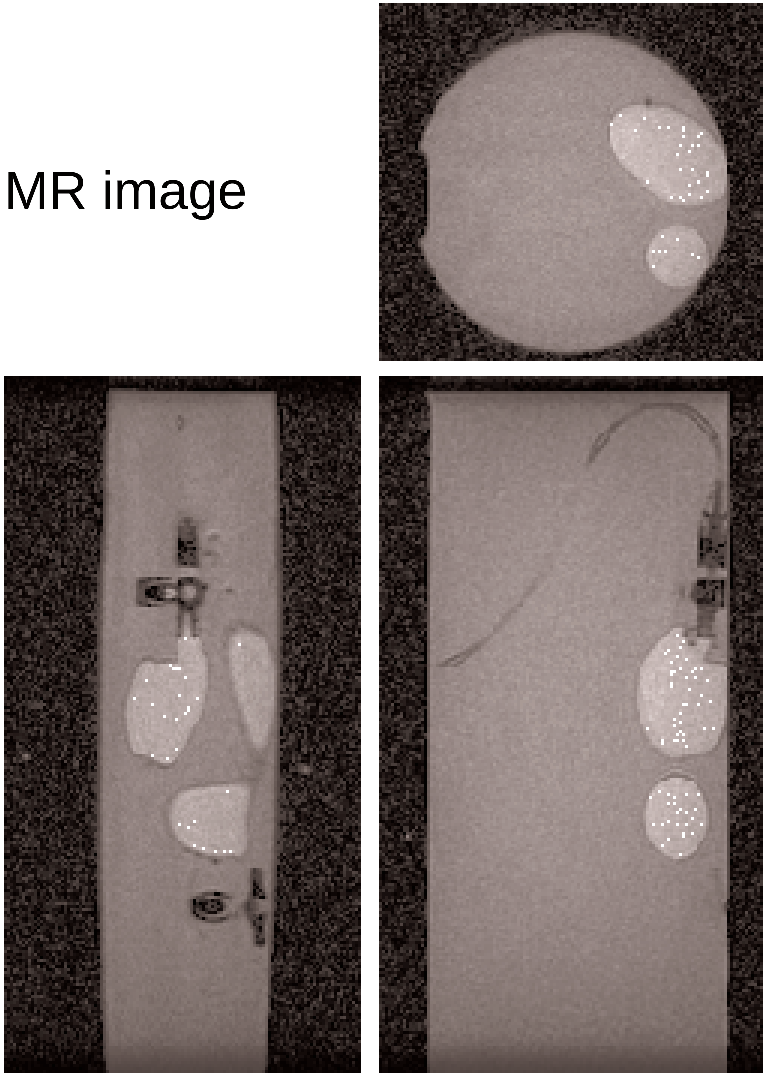

US image, manual init.

Registered US image

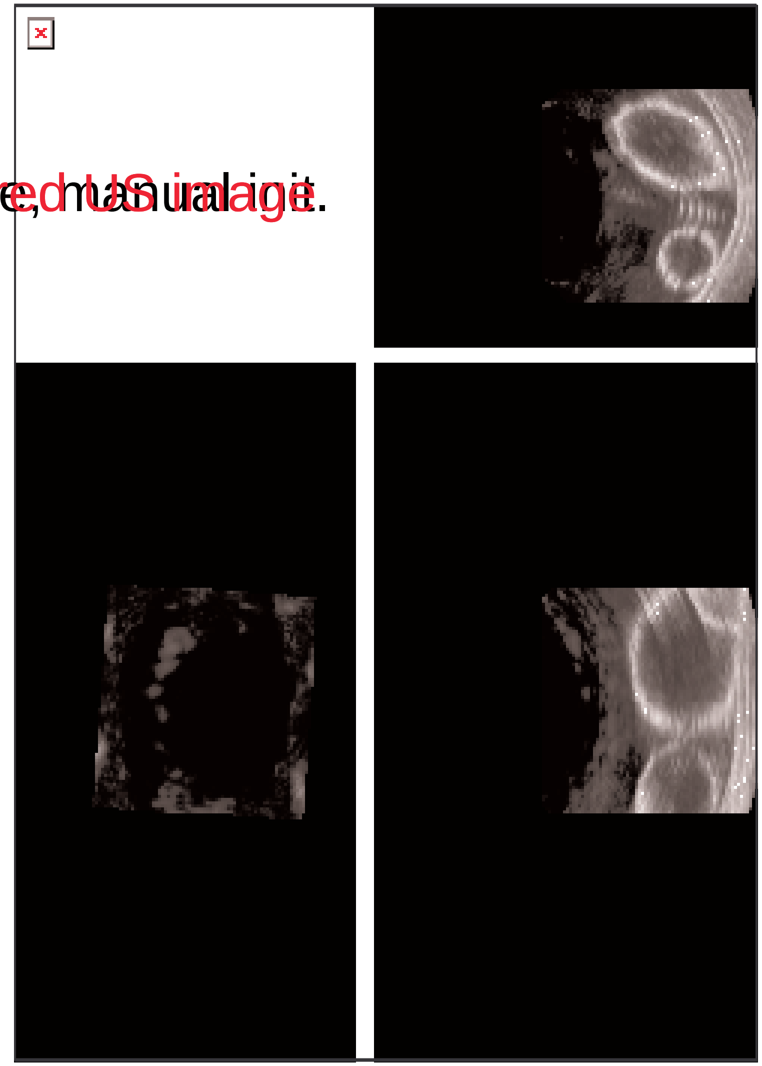

Multiple a posteriori registration

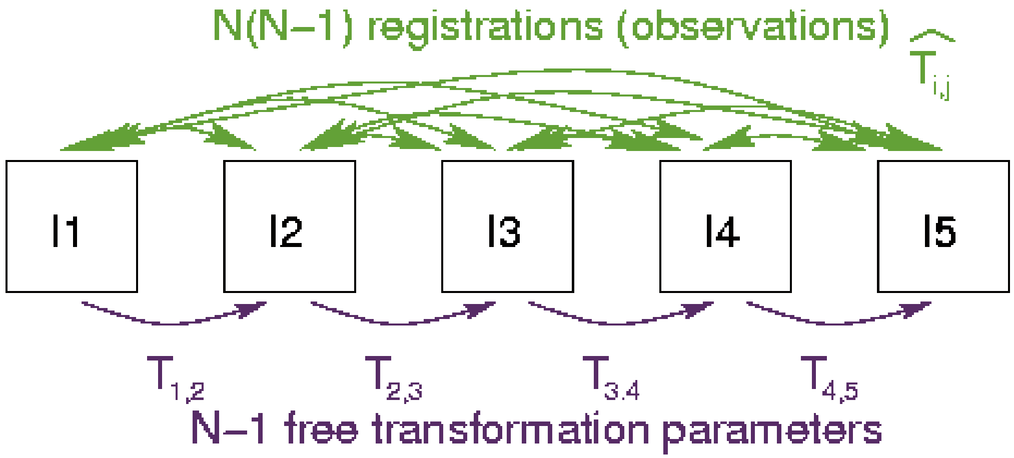

Best explanation of the observations (ML) : $C = \sum_{ij} d^2(T_{ij}, \hat{T}_{ij})$

- LSQ criterion
- Robust Fréchet mean $d^2(T_1, T_2) = \min\left(\mu^2(T_1, T_2), \chi^2\right)$
- Robust initialisation and Newton gradient descent

Result

$$T_{i,j}, \sigma_{rot}, \sigma_{trans}$$

Results on the phantom dataset

Data (varying balloons volumes)

- 8 MR (0.9 x 0.9 x 1.0 mm)
- 8 US (0.4 x 0.4 x 0.4 mm)
- 54 loops

Robustness and repeatability

	Success	var rot (deg)	var trans (mm)
MI	39%	0.40	0.27
CR	52%	0.43	0.25
BCR	**76%**	**0.14**	**0.09**

Consistency of BCR

	var rot (deg)	var trans (mm)	var test (mm)
Multiple MR	0.06	0.1	0.13
Multiple US	0.60	0.4	0.71
Loop	1.62	1.43	2.07
MR/US	**1.06**	**0.97**	**1.37**

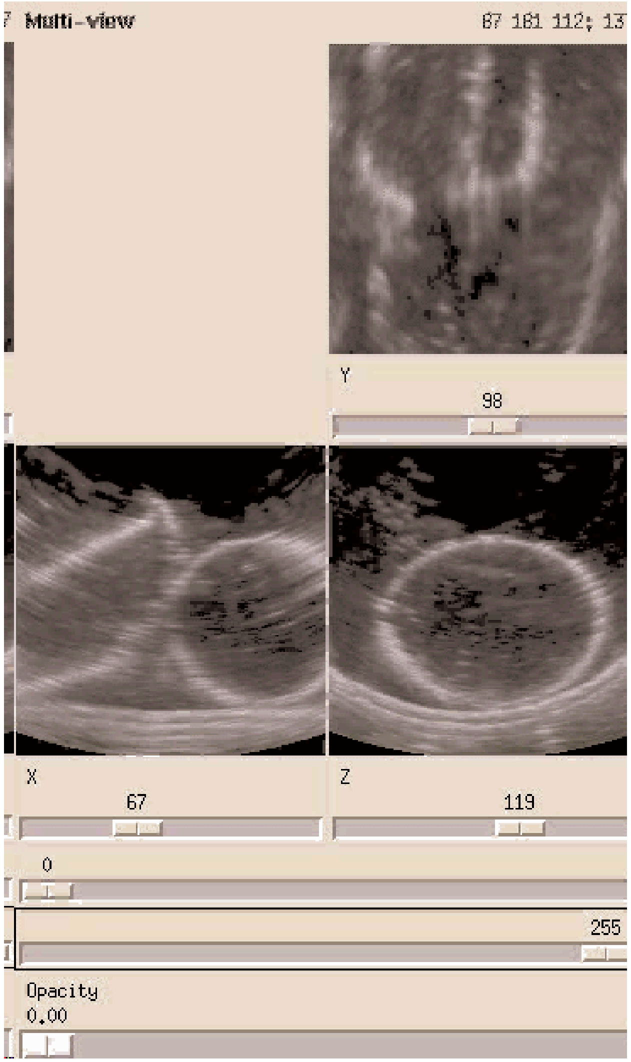

Results on per-operative patient images

Data (per-operative US)

- 2 pre-op MR (0.9 x 0.9 x 1.1 mm)
- 3 per-op US (0.63 and 0.95 mm)
- 3 loops

Robustness and precision

	Success	var rot (deg)	var trans (mm)
MI	29%	0.53	0.25
CR	90%	0.45	0.17
BCR	**85%**	**0.39**	**0.11**

Consistency of BCR

	var rot (deg)	var trans (mm)	var test (mm)
Multiple MR	0.06	0.06	0.10
Loop	2.22	0.82	2.33
MR/US	**1.57**	**0.58**	**1.65**

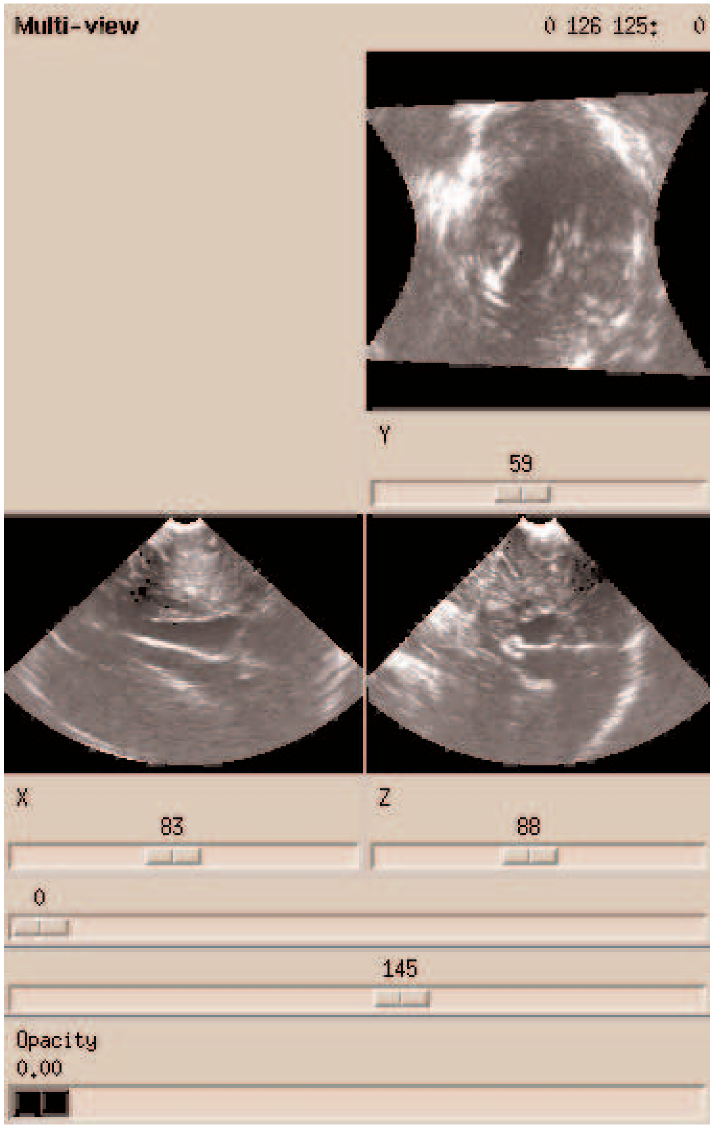

Overview

- ✓ **Statistics on Riemannian manifolds**
- ✓ **Registration performance**
- ⇨ **Tensor computing**
  - ⇨ **Interpolation, filtering, diffusion**
  - ❍ Morphometry of sulcal lines on the brain
- ❍ **Conclusion**

Tensor computing in DTI

Very noisy data

Preprocessing steps

- Filtering
- Regularization
- Robust estimation

Processing steps

- Interpolation / extrapolation
- Statistical comparisons

Can we generalize scalar methods?

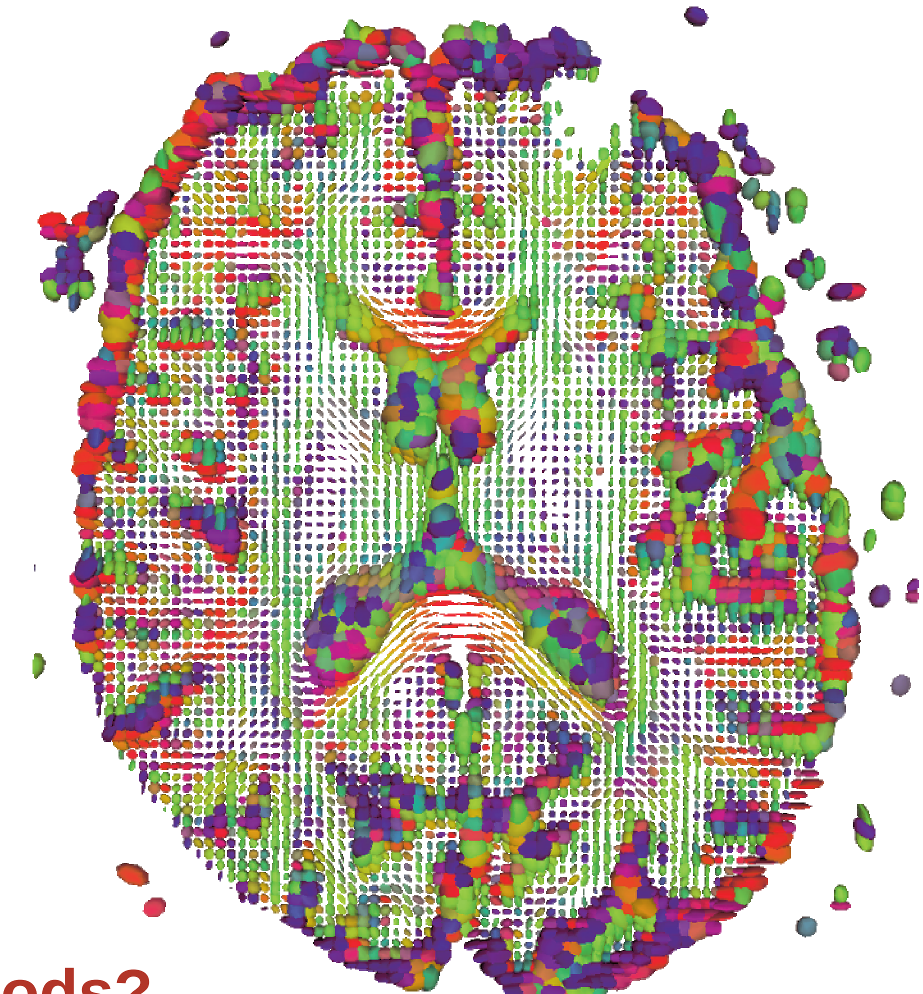

DTI Tensor field (slice of a 3D volume)

Affine Invariant Metric on Tensors

Action of the Linear Group GL_n on Symmetric Matrices

$$\forall A \in GL_n, A * \Sigma = A \Sigma A^T$$

Affine Invariant Distance (positive component)

$$dist(A * \Sigma_1, A * \Sigma_2) = dist(\Sigma_1, \Sigma_2), \forall A \in GL_n$$

Scalar product on $\boldsymbol{T_{Id}M}$:

$$\langle W_1 \mid W_2 \rangle_{Id} \stackrel{def}{=} Tr\left(W_1^T W_2\right)$$

$$W_1, W_2 \in T_{Id}M$$

on $\boldsymbol{T_\Sigma M}$:

$$\langle W_1 \mid W_2 \rangle_\Sigma \stackrel{def}{=} \left\langle \Sigma^{-1/2} * W_1, \Sigma^{-1/2} * W_2 \right\rangle_{Id}$$

X Pennec,P.Fillard,N.Ayache:Riemannian Tensor Computing, RR-5255, INRIA, July 2004

Exponential and Logarithmic Maps

Geodesics $\Gamma_{Id,W}(t) = \exp(tW)$

- Exponential Map :

$$\exp_\Sigma(\overrightarrow{\Sigma\Psi}) = \Sigma^{1/2}\exp(\Sigma^{-1/2}.\overrightarrow{\Sigma\Psi}.\Sigma^{-1/2})\Sigma^{1/2}$$

- Logarithmic Map :

$$\overrightarrow{\Sigma\Psi} = \log_\Sigma(\Psi) = \Sigma^{1/2}\log(\Sigma^{-1/2}.\Psi.\Sigma^{-1/2})\Sigma^{1/2}$$

$$dist(\Sigma,\Psi)^2 = \left\langle \overrightarrow{\Sigma\Psi} \mid \overrightarrow{\Sigma\Psi} \right\rangle_\Sigma = \left\| \log(\Sigma^{-1/2}.\Psi.\Sigma^{-1/2}) \right\|_{L_2}^2$$

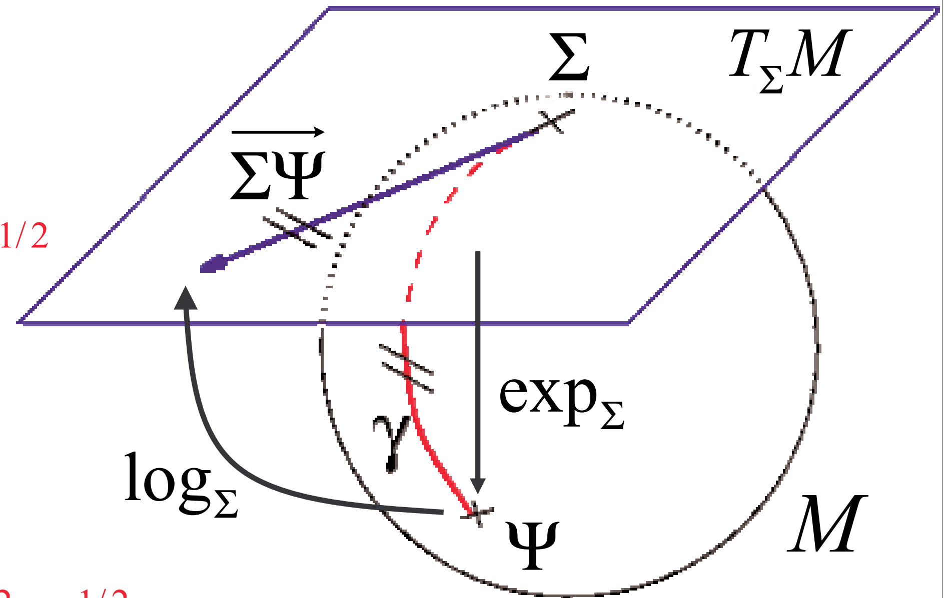

Linear vs. Riemannian Interpolation: walking along geodesics

Interpolation of the coefficients:

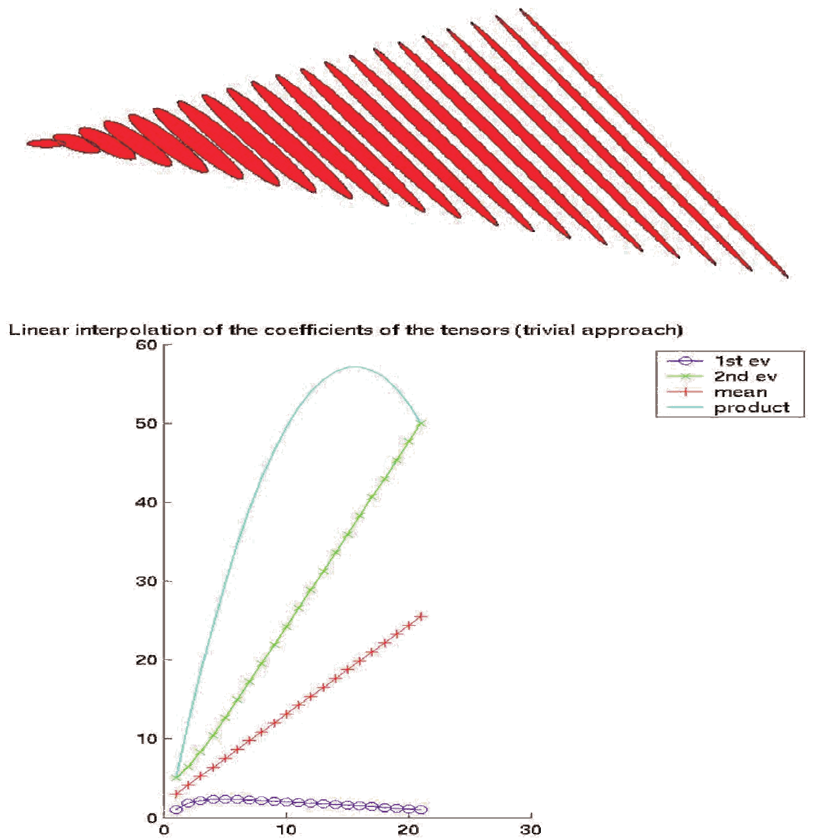

Interpolation achieved with the Riemannian metric:

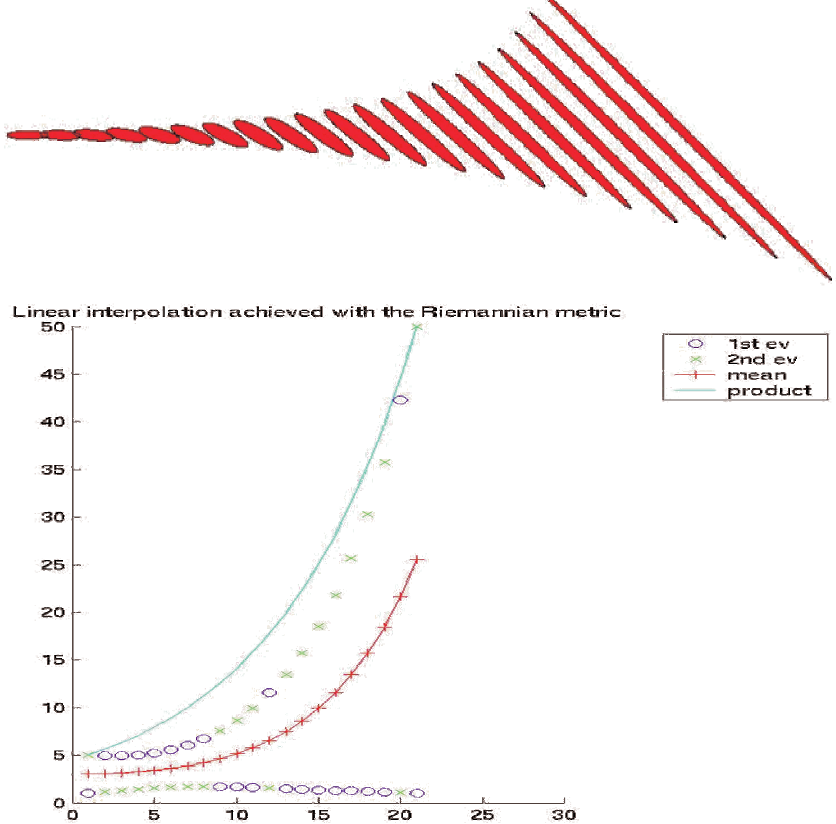

X Pennec,P.Fillard,N.Ayache:Riemannian Tensor Computing, RR-5255, INRIA, July 2004

General interpolation

$$\Sigma(x) = \min \sum_{i=1}^{n} w_i(x) \; dist(\Sigma, \Sigma_i)^2$$

Bilinear interpolation: weighted mean with bi-linear weights

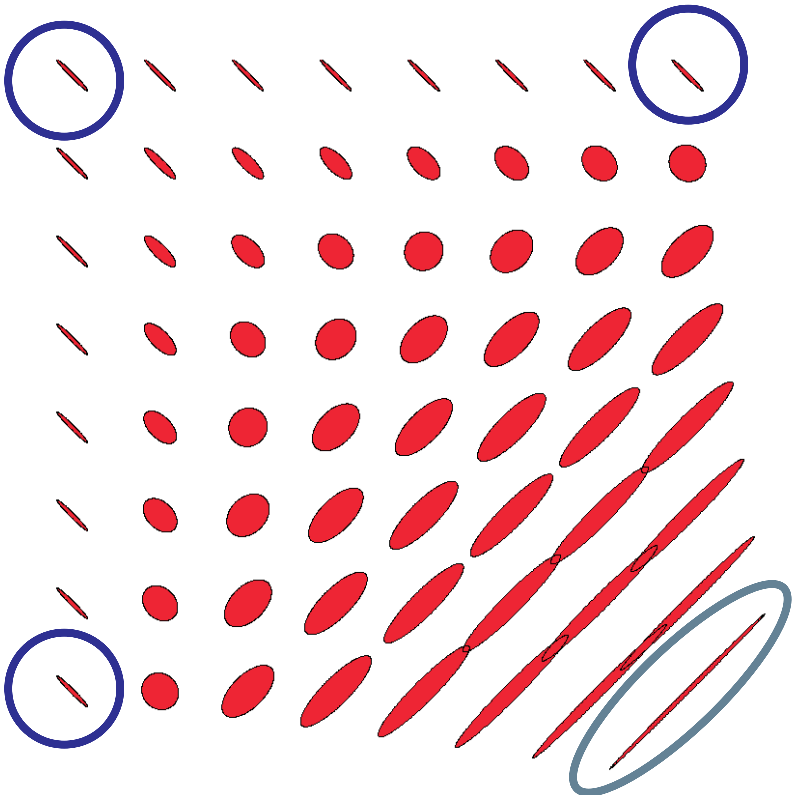

Coefficients

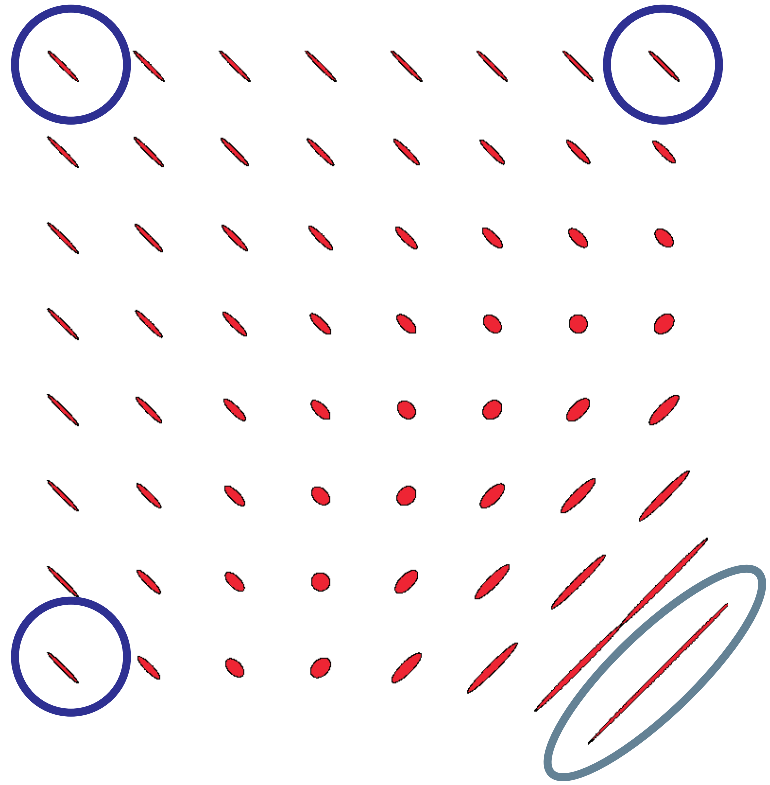

Riemannian metric

General interpolation

$$\Sigma(x) = \min \sum_{i=1}^{n} w_i(x) \; dist(\Sigma, \Sigma_i)^2$$

Trilinear interpolation: weighted mean with tri-linear

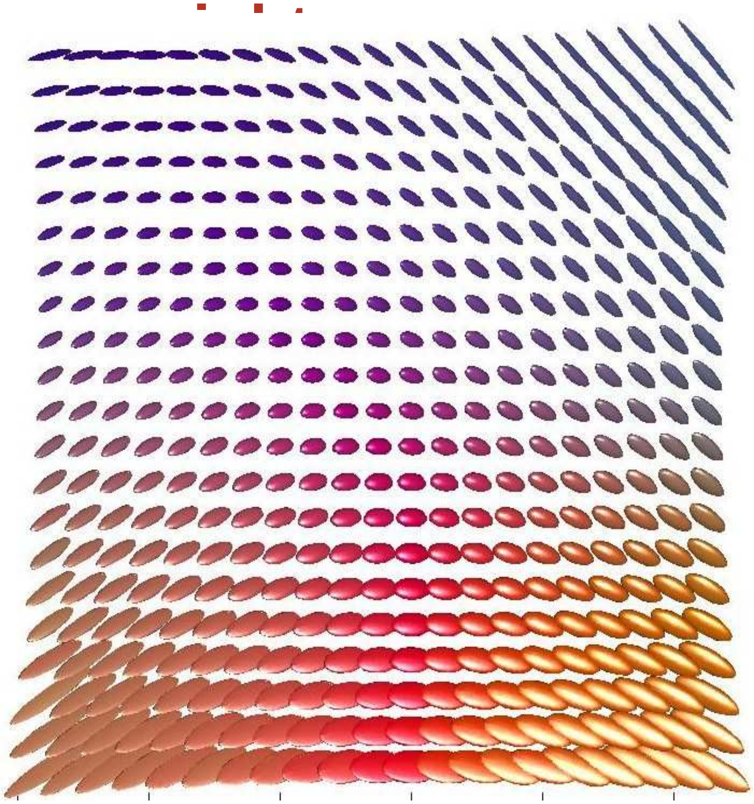

Riemannian metric

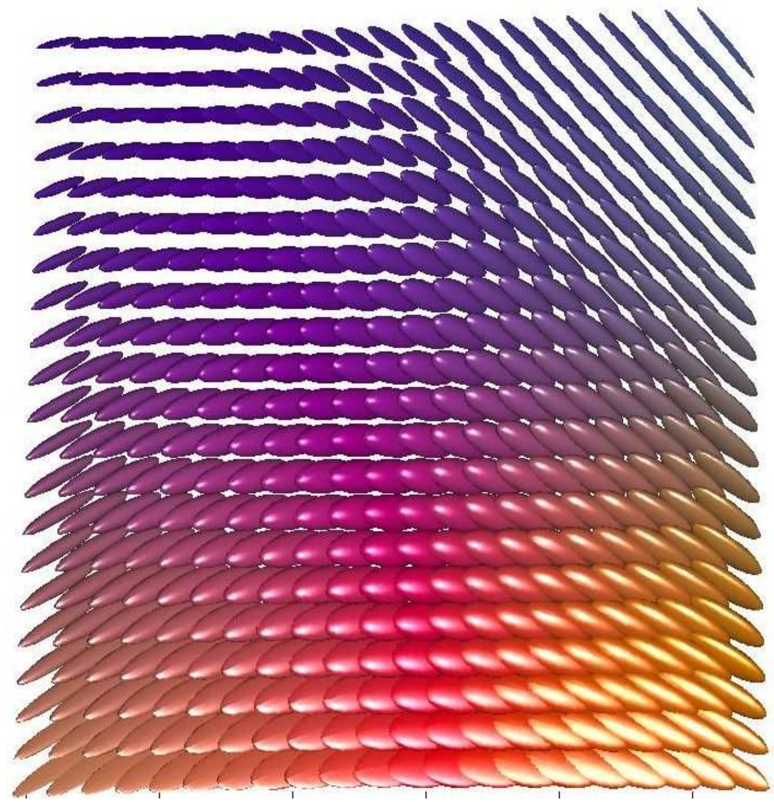

Coefficients

Gaussian filtering: Gaussian weighted mean

$$\Sigma(x) = \min \sum_{i=1}^{n} G_\sigma(x - x_i) \; dist\,(\Sigma, \Sigma_i)^2$$

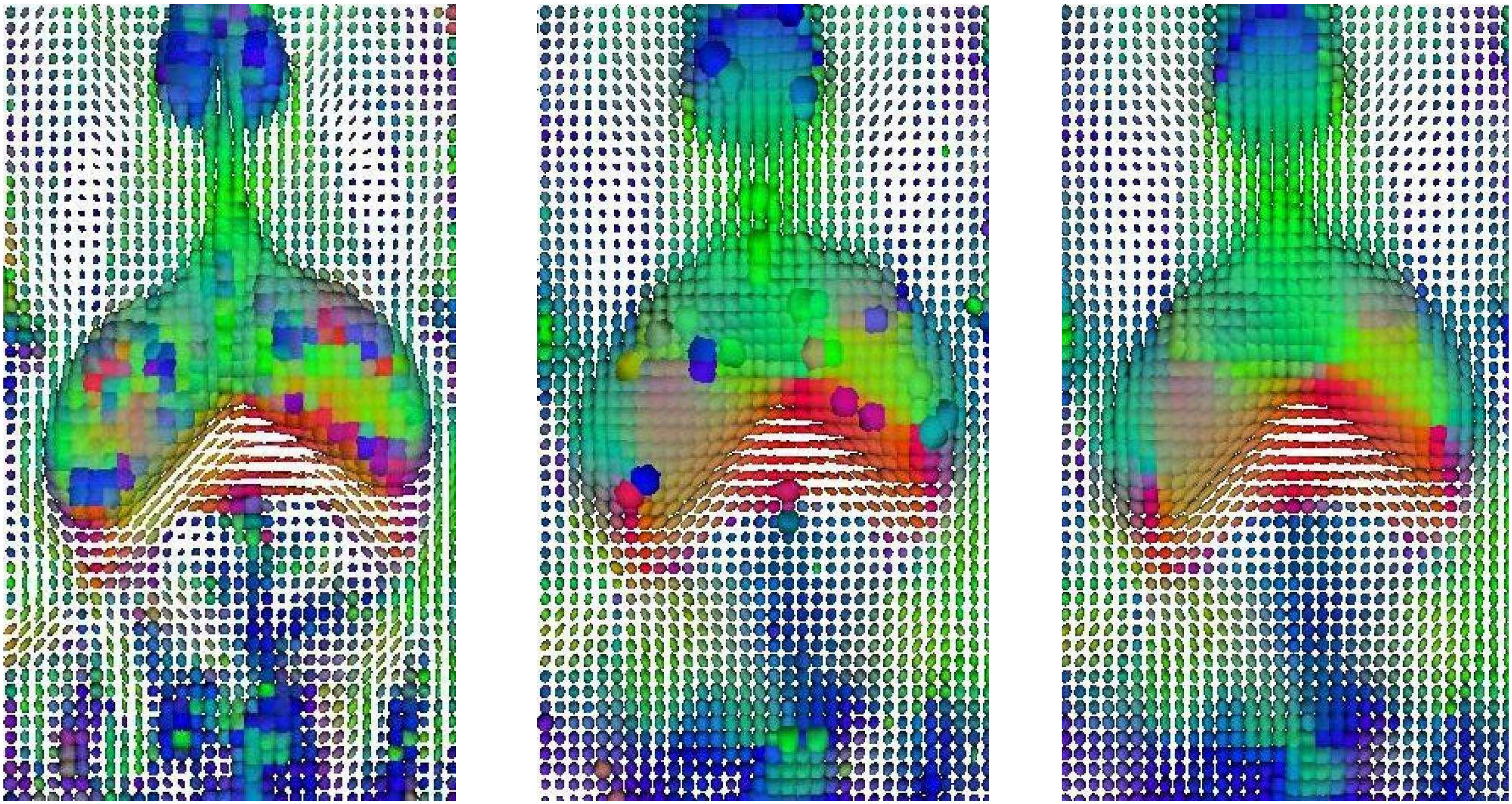

Raw Coefficients σ=2 Riemann σ=2

Harmonic and Anisotropic filtering

Harmonic regularization

$$C(\Sigma) = \int_{\Omega} \left\| \nabla \Sigma(x) \right\|^2 dx$$

$$\nabla C(x) = -2\Delta\Sigma(x) = -2\sum_{u} \frac{\overrightarrow{\Sigma(x)\Sigma(x+u)}}{\left\| u \right\|^2}$$

Anisotropic regularization

- Penalize diffusion in the directions where the direction derivative is strong

$$g(\mathrm{x}) = \exp\left(-\mathrm{x}^2 / \kappa^2\right)$$

$$\Delta_g \Sigma(x) = \sum_{u} \frac{g\left(\partial_u \Sigma(x)\right)\ \partial_u^2 \Sigma(x)}{\left\| u \right\|^2} = \sum_{u} g\left(\frac{\left\| \overrightarrow{\Sigma(x)\Sigma(x+u)} \right\|_{\Sigma(x)}}{\left\| u \right\|} \right) \frac{\overrightarrow{\Sigma(x)\Sigma(x+u)}}{\left\| u \right\|^2}$$

Harmonic and Anisotropic filtering

Classical gradient descent

$$\Sigma(x,t+dt) = \Sigma(x,t) - dt\,\nabla C(\Sigma) = \Sigma(x,t) + dt\,\Delta\Sigma(x,t)$$

- Unstable

Intrinsic gradient descent

$$\Sigma(x,t+dt) = \exp_{\Sigma(x,t)}(-dt.\nabla C(\Sigma)) = \exp_{\Sigma(x,t)}(dt.\Delta_g \Sigma(x,t))$$

- Ensures strict positivity

Anisotropic filtering

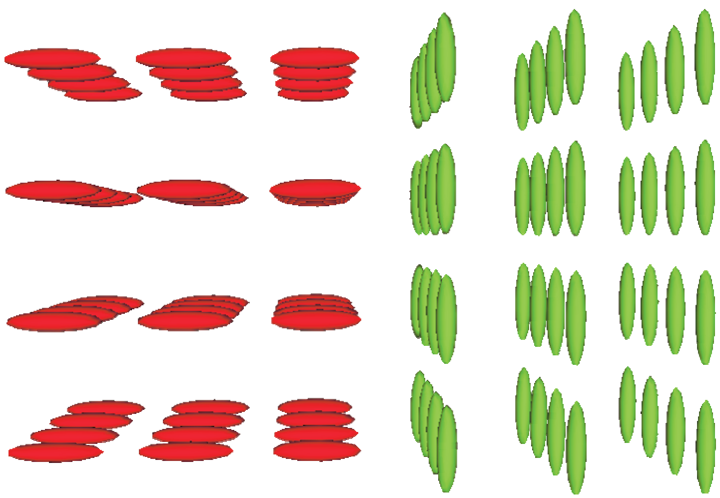

Initial

Noisy

Recovered

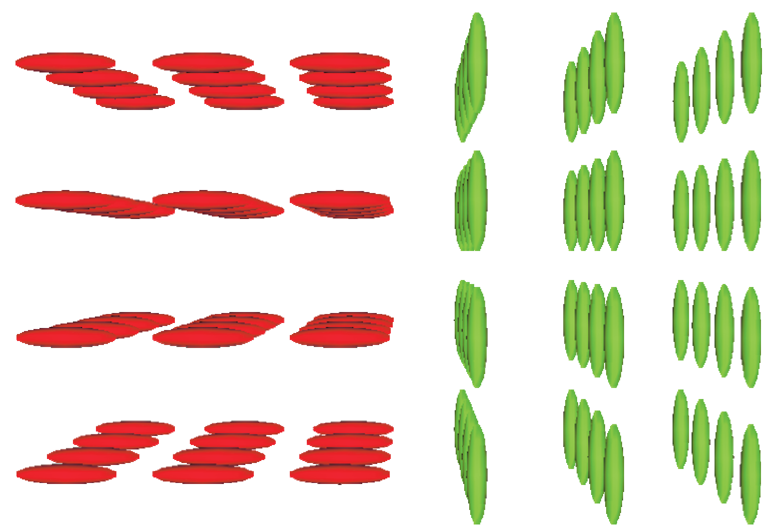

Anisotropic filtering

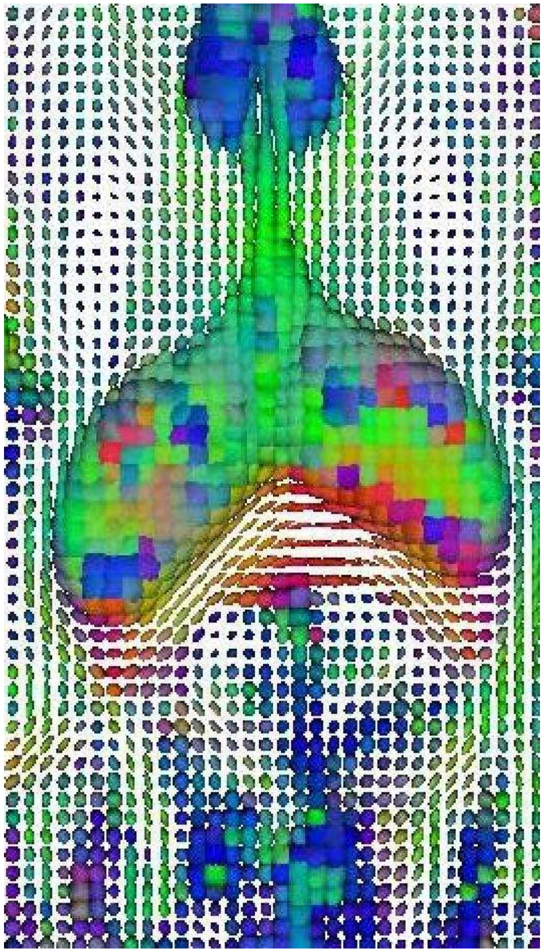

Raw

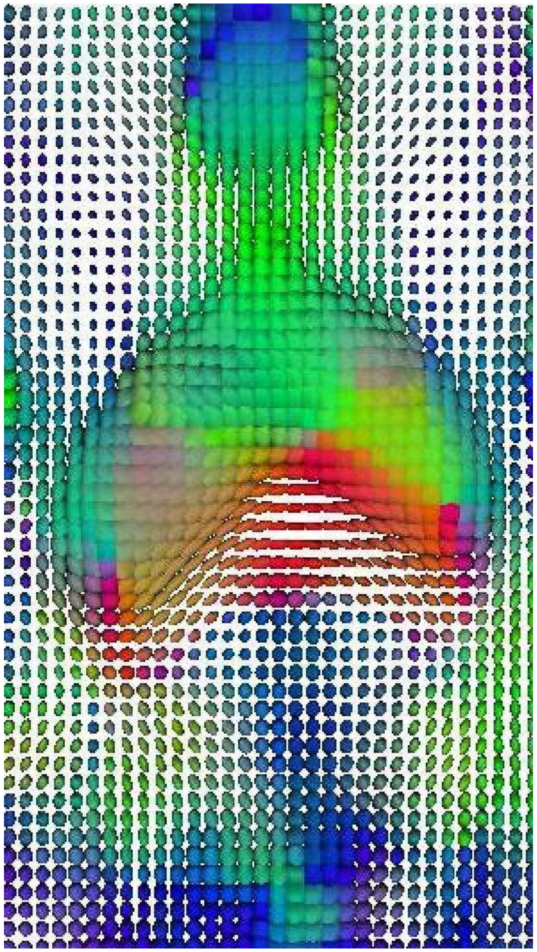

Riemann Gaussian

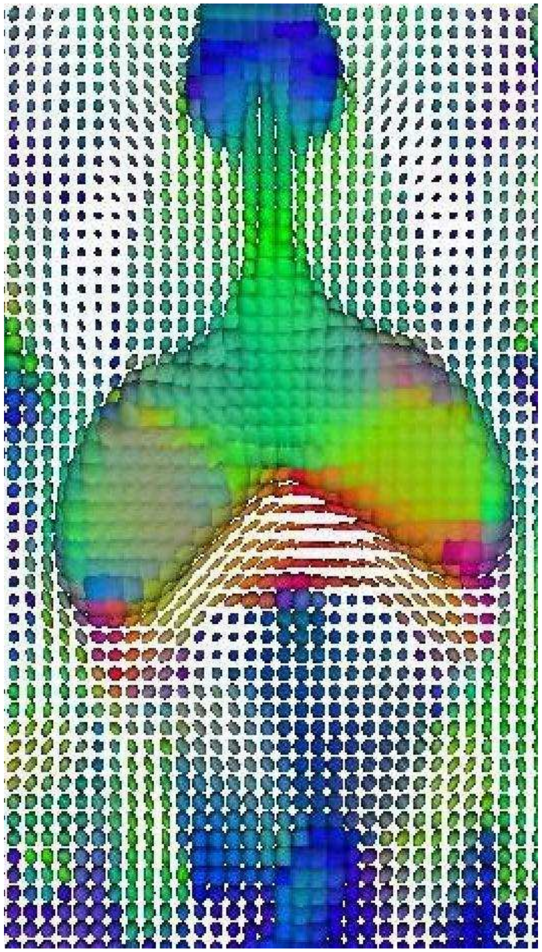

Riemann anisotropic

Extrapolation by Diffusion

sources = tensors at given positions

smooth extrapolation

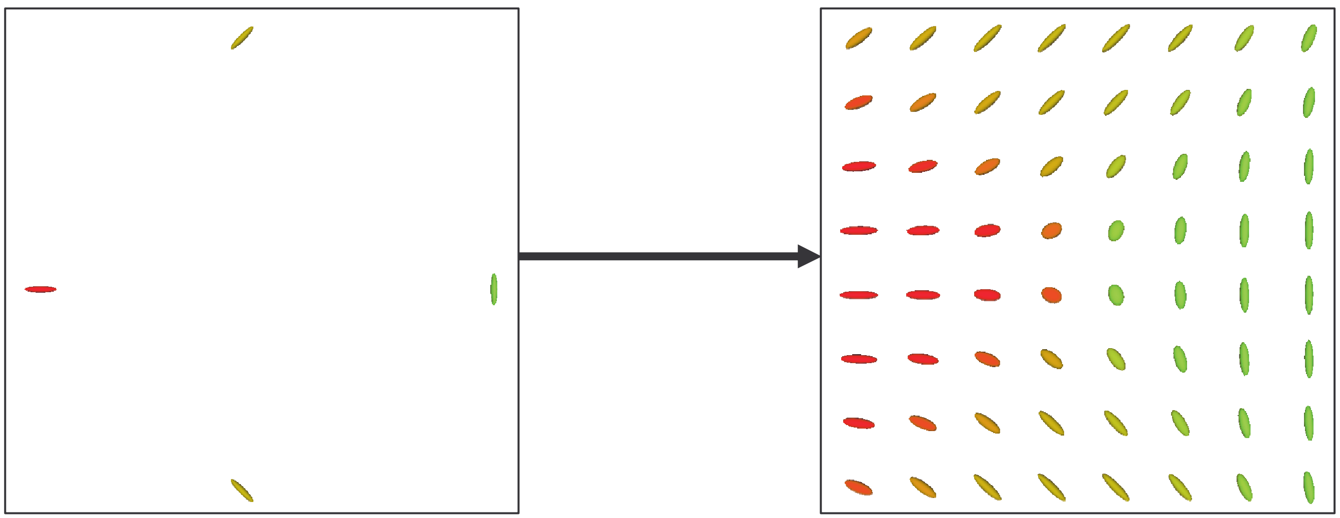

Extrapolation by Diffusion

$$C(\Sigma) = \frac{1}{2}\int_{\Omega}\sum_{i=1}^{n} G_{\sigma}(x - x_i)\, dist(\Sigma(x), \Sigma_i)^2\, dx + \frac{\lambda}{2}\int_{\Omega}\left\|\nabla\Sigma\right\|^2$$

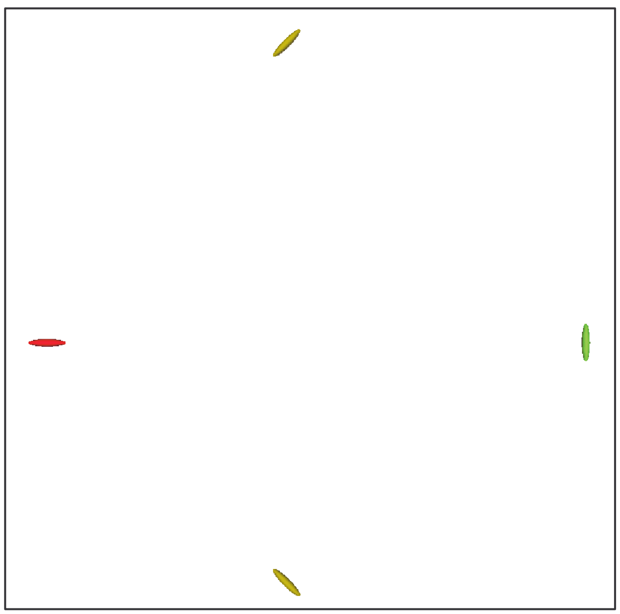

Original Tensor Data

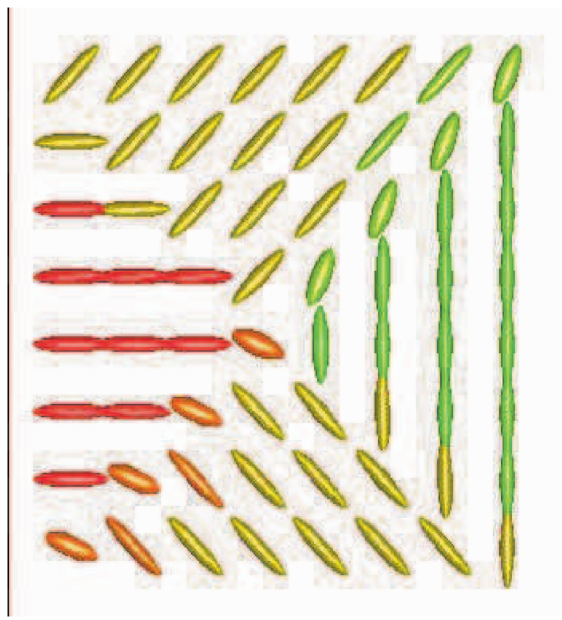

DiffusionWithout data attachement

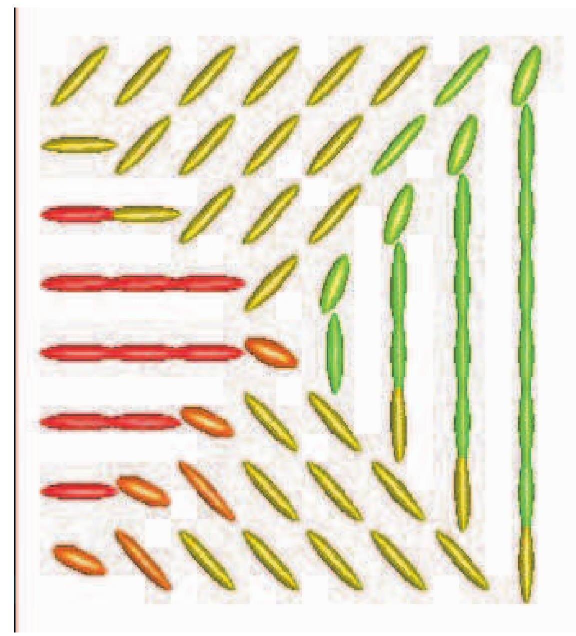

Diffusion with data attachement

Overview

- ✓ **Statistics on Riemannian manifolds**
- ✓ **Registration performance**
- ⇨ **Tensor computing**
  - ✓ Motivation for an invariant metric
  - ✓ Interpolation, filtering, diffusion
  - ⇨ **Morphometry of sulcal lines on the brain**
- ❍ **Conclusion**

Morphometry of Sucal Lines

Goal:

- Learn local brain variability from sulci
- Better constrain inter-subject registration
- Correlate this variability with age, pathologies

Collaborative work between Epidaure (INRIA) and LONI (UCLA)
V. Arsigny, N. Ayache, P. Fillard, X. Pennec and P. Thompson

Fillard-Arsigny-Pennec-Ayache-Thompson, submitted to IPMI'05

Computation of Average Sulci

Alternate minimization of global variance

- Dynamic programming to match the mean to instances
- Gradient descent to compute the mean curve position

red : mean curve
green: ~80 instances of 72 sulci

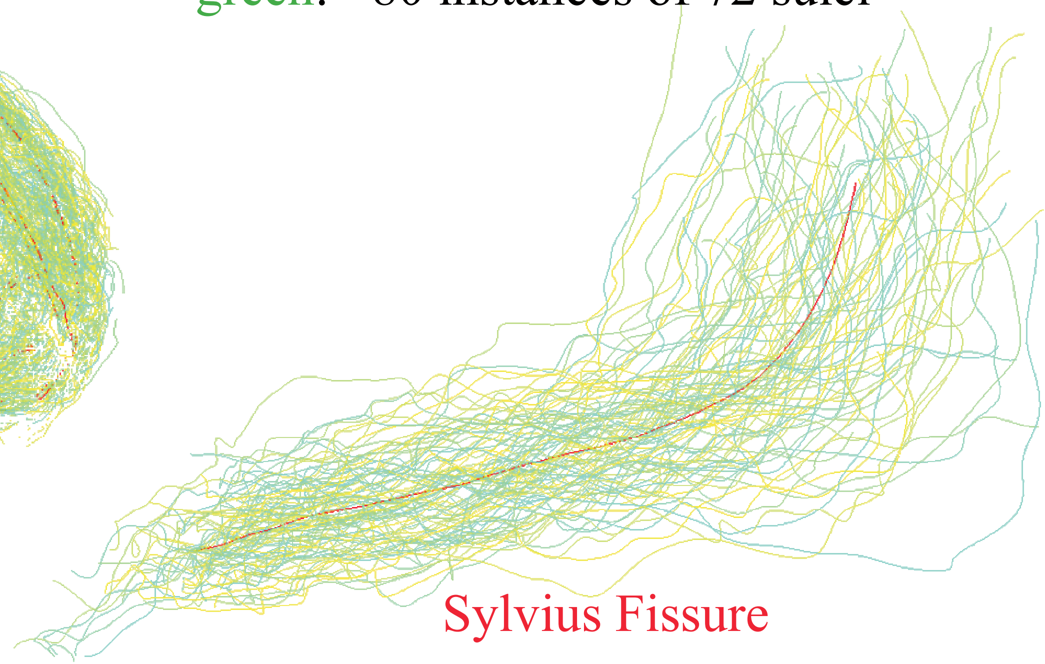

Anatomical variability

Variance along the mean sulci

- Red (low) to blue (high)

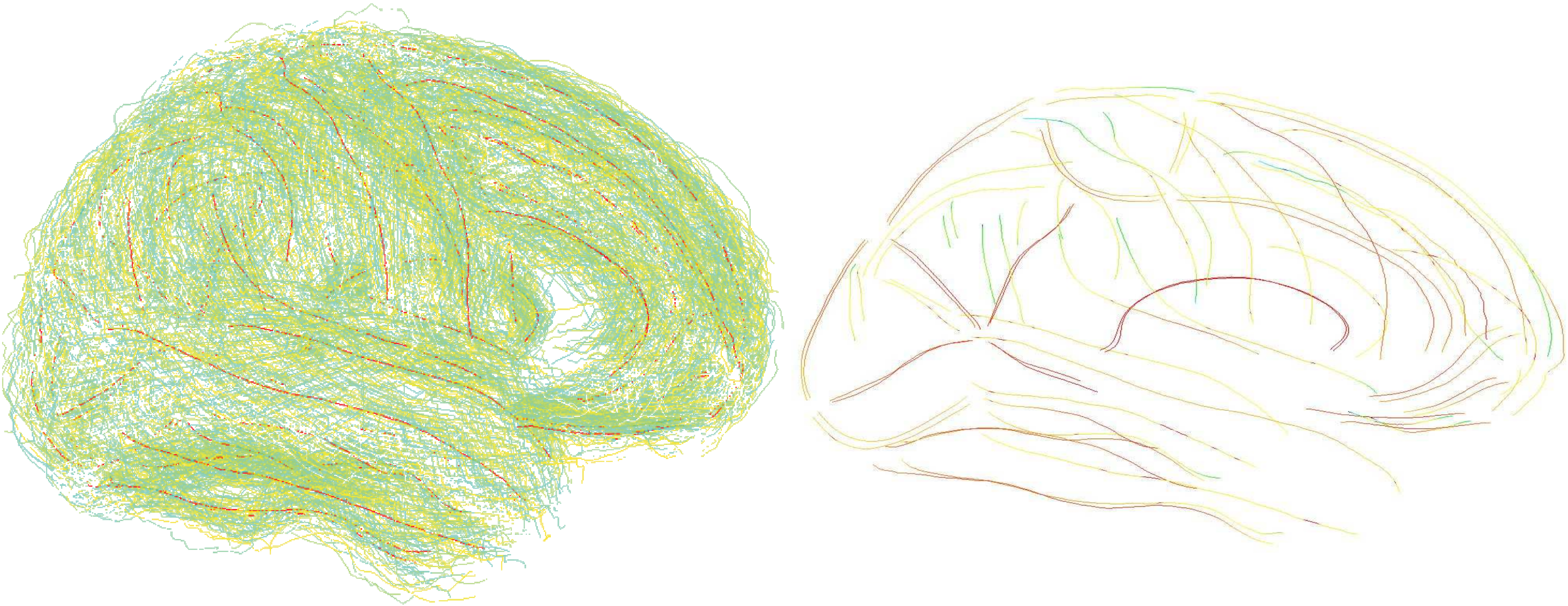

Extraction of Covariance Tensors

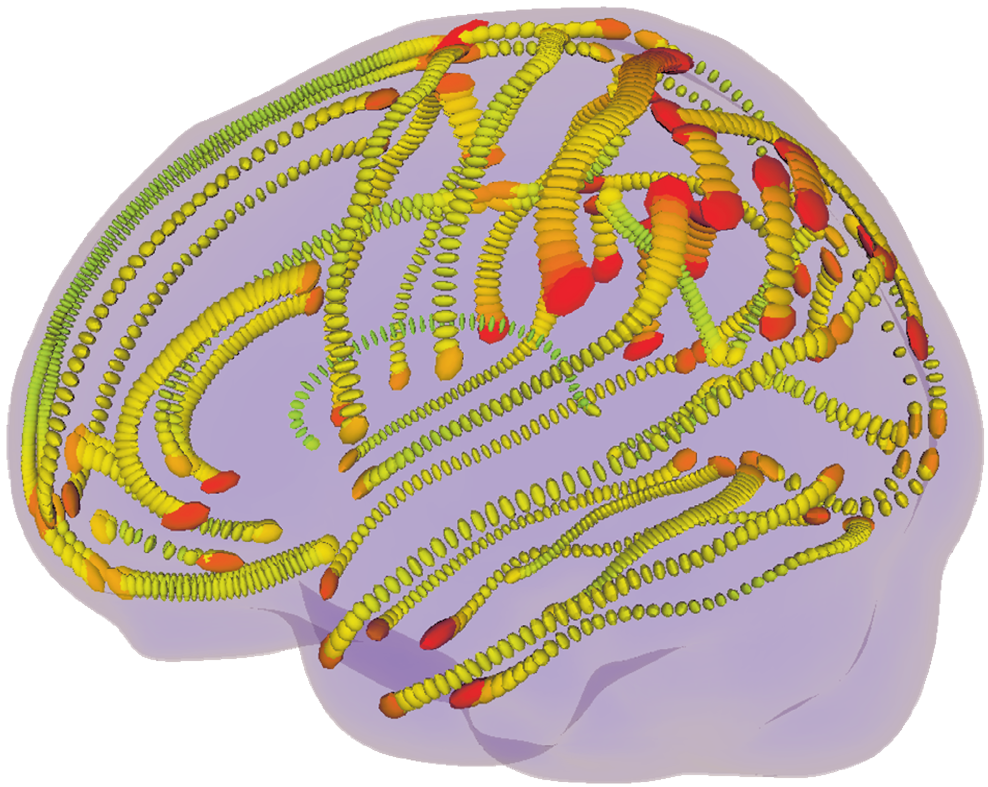

Color codes Trace

Currently:

80 instances of 72 sulci

About 1250 tensors

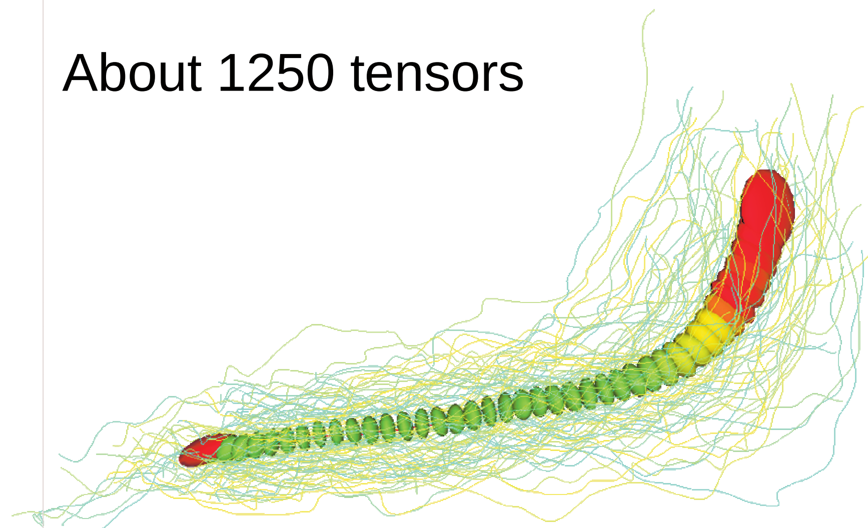

Covariance Tensors
along Sylvius Fissure

Compressed Tensor Representation

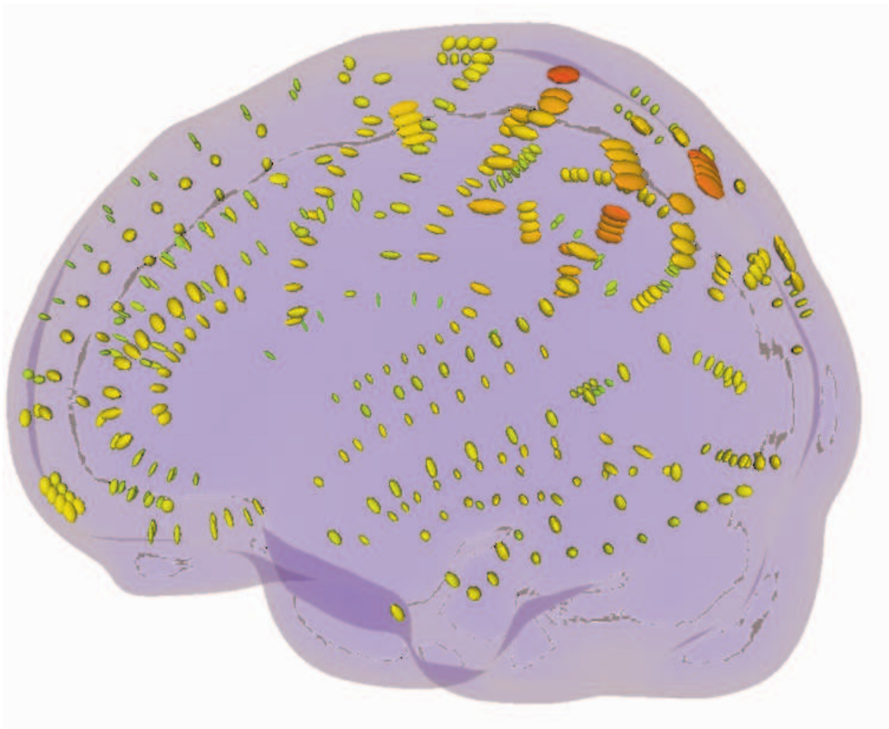

Representative Tensors (250)

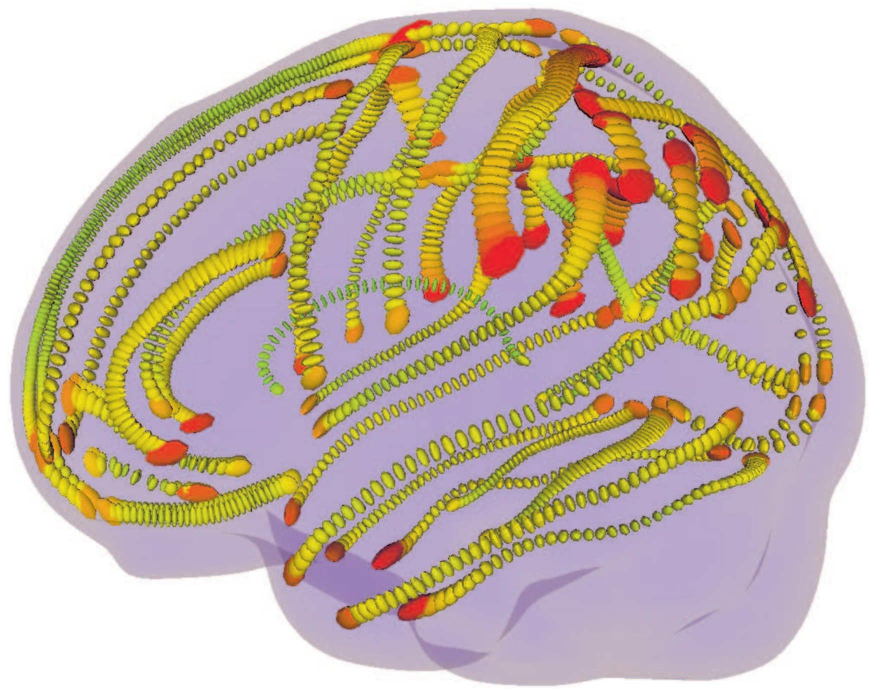

Reconstructed Tensors (~1250)
(Riemannian Interpolation)

Original Tensors (1250)

Variability Tensors

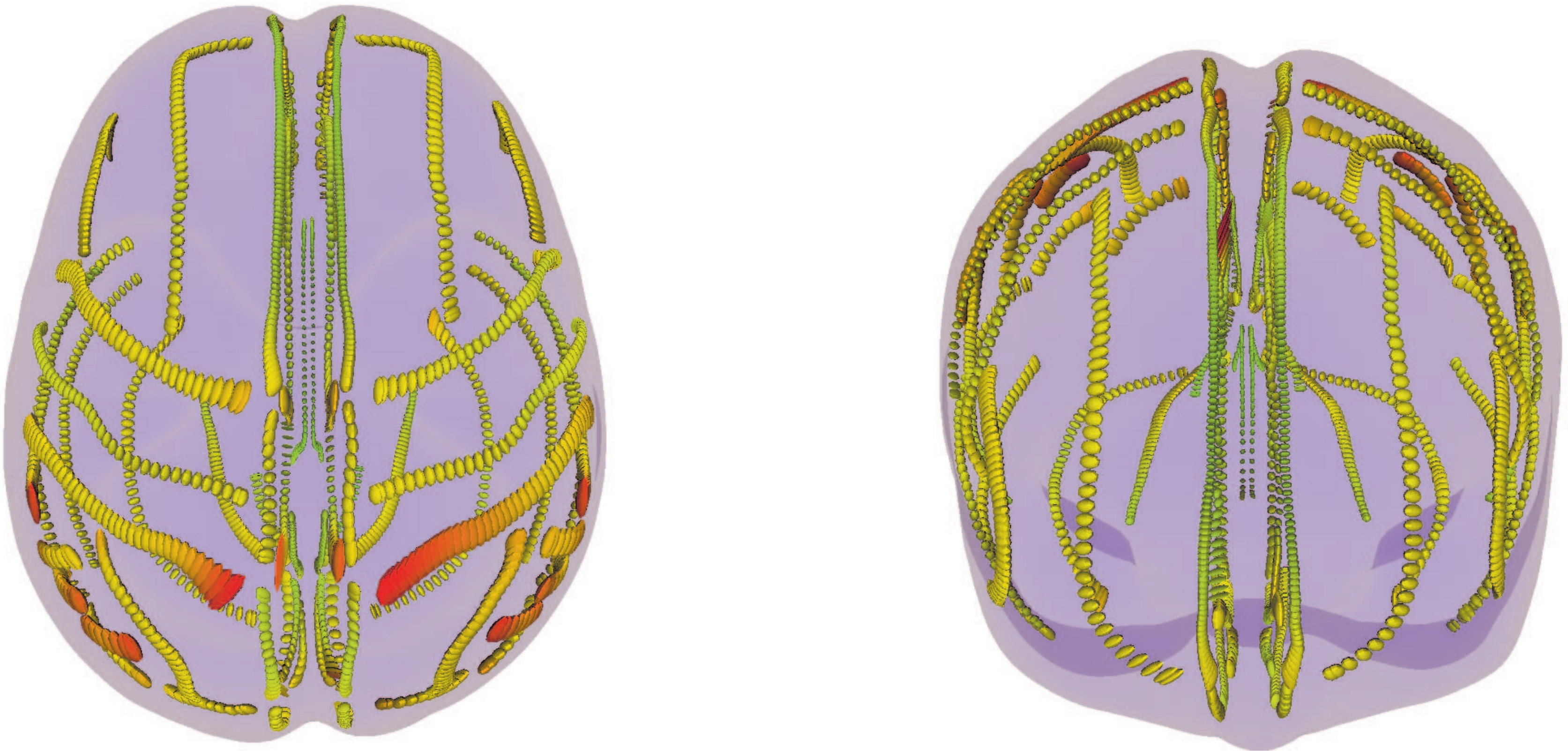

Color codes tensor trace

Quantitative comparison: Asymmetry Measure

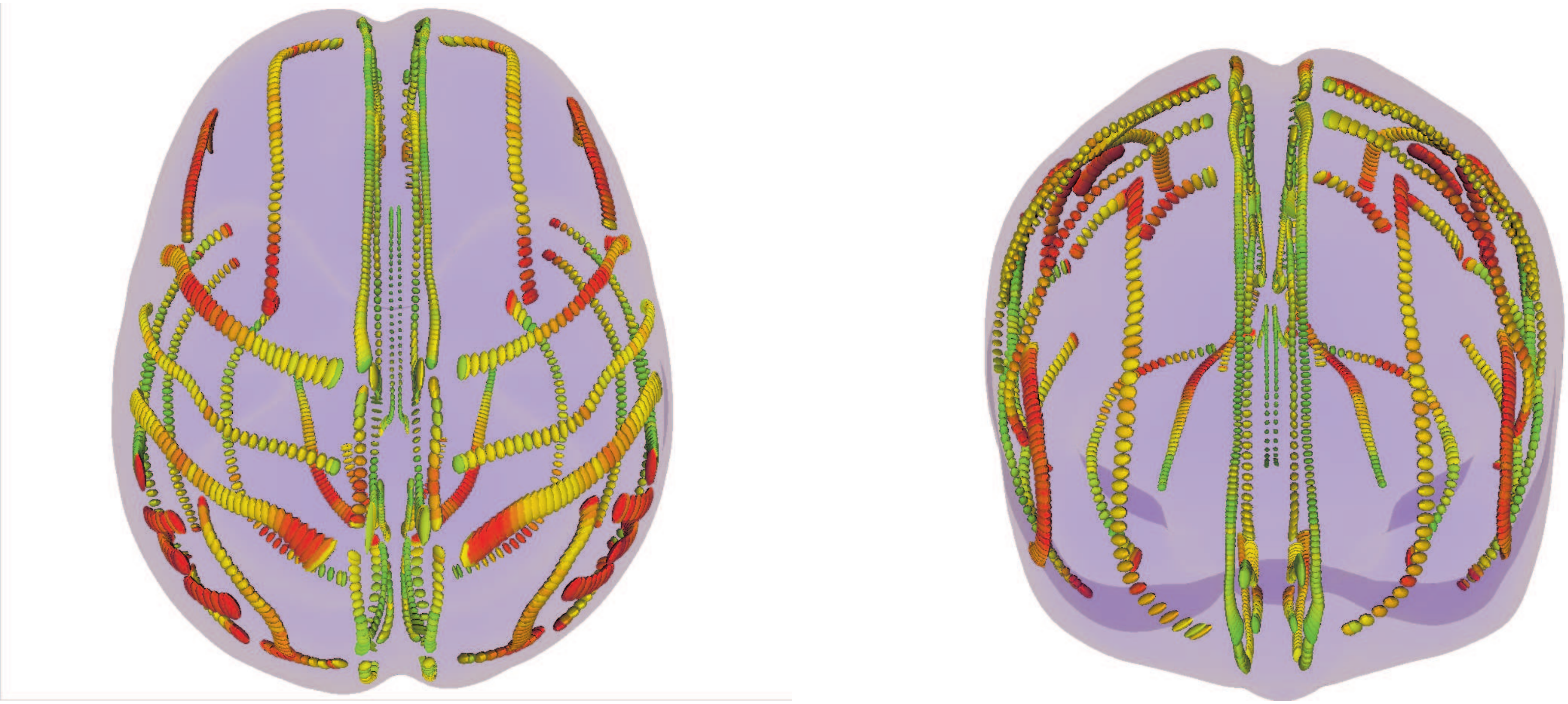

Color Codes Distance between “symmetric” tensors

$$dist(\Sigma,\Sigma')^2 = \left\langle \overrightarrow{\Sigma\Sigma'} \mid \overrightarrow{\Sigma\Sigma'} \right\rangle_{\Sigma} = \left\| \log(\Sigma^{-1/2}.\Sigma'.\Sigma^{-1/2}) \right\|_{L_2}^2$$

Full Brain extrapolation of the variability

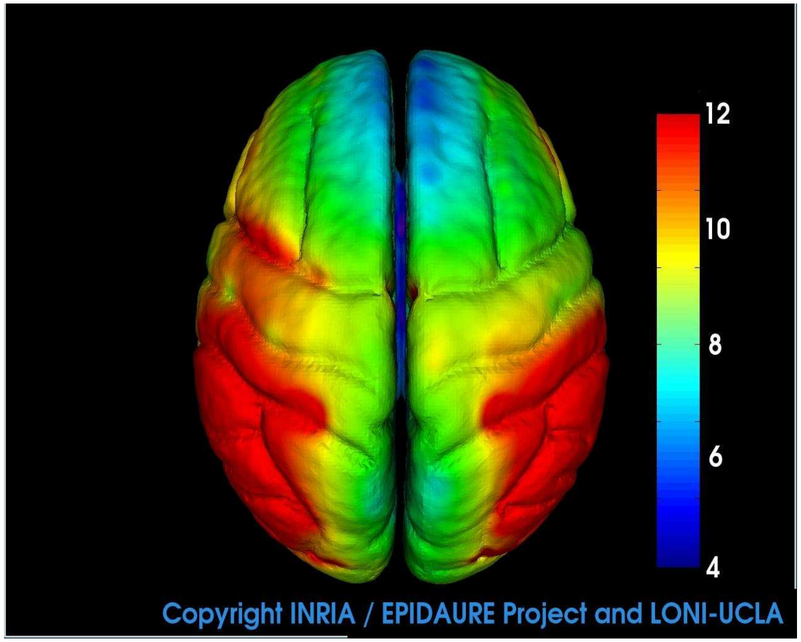

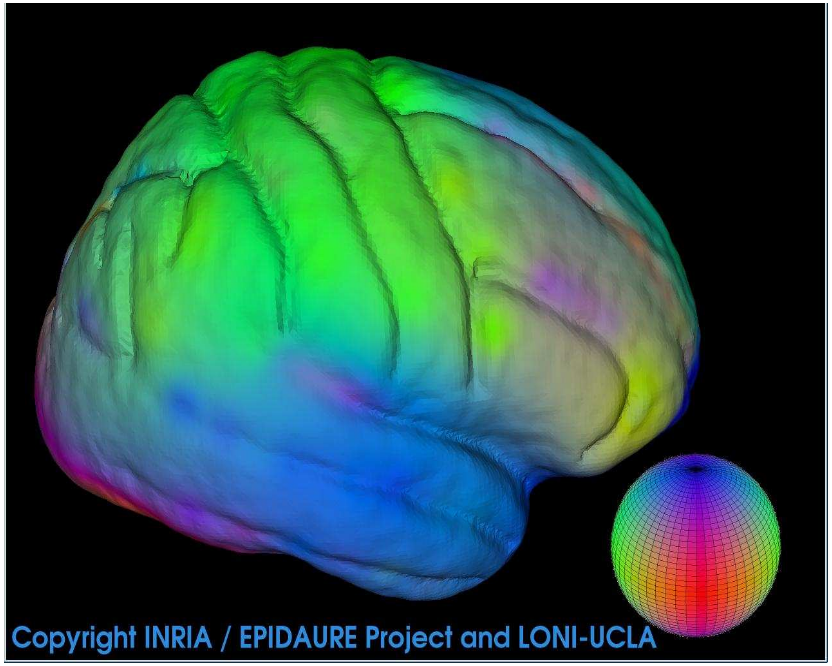

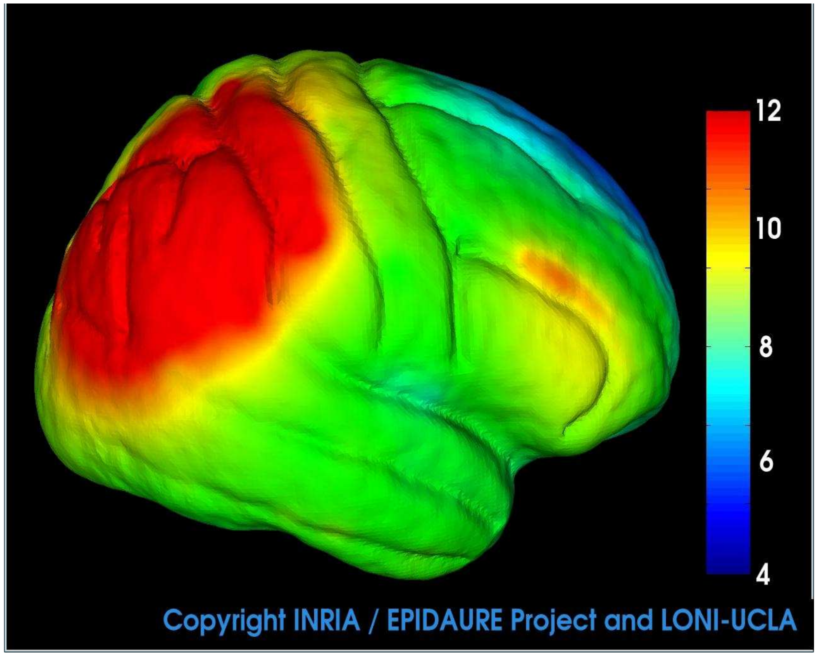

Overview

- ✓ **Statistics on Riemannian manifolds**
- ✓ **Registration performance**
- ✓ **Tensor computing**
- ⇨ **Conclusion**

Conclusion : geometry and statistics

A Statistical computing framework on "simple" manifolds

- Mean, Covariance, statistical tests…
- Interpolation, diffusion, filtering…
- How to choose the metric?

Extend to more complex groups and manifolds

- Deformations (Trouvé, Younes, Miller)
- Shapes (Kendall, Olsen)

Spatially extended features (curves, surfaces, volumes…)

- Homology assumption (mixtures ?)
- Spatial correlation between neighbors
- Probability density for curves and surfaces

Applications of Riemannian Computing

Registration

- Performance evaluation
- Introducing a-priori distributions
- Statistical deformations

Diffusion tensor imaging

- Regularization for fiber tracts estimation
- Registration (atlases)

Variability of the brain

- Learn Variability from Large Group Studies
- Statistical Comparisons between Groups
- Improve Inter-Subject Registration

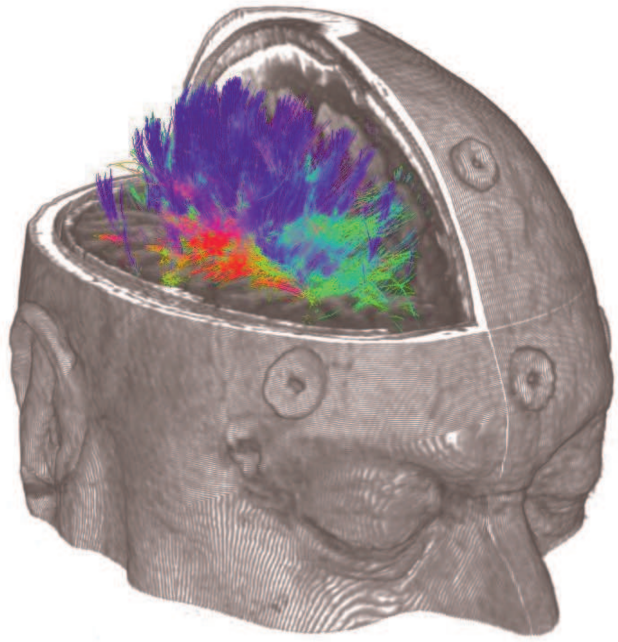

References

- **Statistics on Manifolds**
  - X. Pennec. **Probabilities and Statistics on Riemannian Manifolds: A Geometric approach**. Research Report 5093, INRIA, January 2004. Submitted to Int. Journal of Mathematical Imaging and Vision. http://www.inria.fr/rrrt/rr-5093.html
  - X. Pennec and N. Ayache. **Uniform distribution, distance and expectation problems for geometric features processing.** Journal of Mathematical Imaging and Vision, 9(1):49-67, July 1998.
- **Registration of medical images**
  - X. Pennec, N. Ayache, and J.-P. Thirion. **Landmark-based registration using features identified through differential geometry.** In I. Bankman, editor, Handbook of Medical Imaging, chapter 31, pages 499-513. Academic Press, September 2000.
  - X. Pennec and J.-P. Thirion. **A Framework for Uncertainty and Validation of 3D Registration Methods based on Points and Frames.** Int. Journal of Computer Vision, 25(3):203-229, 1997.
- **Tensor Computing**
  - X. Pennec, P. Fillard, and Nicholas Ayache. **A Riemannian Framework for Tensor Computing.** Research Report 5255, INRIA, July 2004. Submitted to the Int. Journal of Computer Vision. http://www.inria.fr/rrrt/rr-5255.html
  - P. Fillard, V. Arsigny, X. Pennec, P. Thompson, and N. Ayache. **Modeling of the Brain Variability**. Submitted to IPMI'05, 2005.